Contrib Mineral Petrol (2015) 169:44
DOI 10.1007/s00410-015-1135-6

ORIGINAL PAPER

Constraints on the thermal evolution of the Adriatic margin during Jurassic continental break-up: U–Pb dating of rutile from the Ivrea–Verbano Zone, Italy

Tanya A. Ewing[1,2] · Daniela Rubatto[1] · Marco Beltrando[3] · Jörg Hermann[1]

Received: 5 November 2014 / Accepted: 30 March 2015 / Published online: 23 April 2015

Abstract The Ivrea–Verbano Zone (IVZ), northern Italy, exposes an attenuated section through the Permian lower crust that records high-temperature metamorphism under lower crustal conditions and a protracted history of extension and exhumation associated partly with the Jurassic opening of the Alpine Tethys ocean. This study presents SHRIMP U–Pb geochronology of rutile from seven granulite facies metapelites from the base of the IVZ, collected from locations spanning ~35 km along the strike of Paleozoic fabrics. Rutile crystallised during Permian high-temperature metamorphism and anatexis, yet all samples give Jurassic rutile U–Pb ages that record cooling through 650–550 °C. Rutile age distributions are dominated by a peak at ~160 Ma, with a subordinate peak at ~175 Ma. Both ~160 and ~175 Ma age populations show excellent agreement between samples, indicating that the two distinctive cooling stages they record were synchronous on a regional scale. The ~175 Ma population is interpreted to record cooling in the footwall of rift-related faults and shear zones, for which widespread activity in the Lower Jurassic has been documented along the western margin of the Adriatic plate. The ~160 Ma age population postdates the activity of all known rift-related structures within the Adriatic margin, but coincides with extensive gabbroic magmatism and exhumation of sub-continental mantle to the floor of the Alpine Tethys, west of the Ivrea Zone. We propose that this ~160 Ma early post-rift age population records regional cooling following episodic heating of the distal Adriatic margin, likely related to extreme lithospheric thinning and associated advection of the asthenosphere to shallow levels. The partial preservation of the ~175 Ma age cluster suggests that the post-rift (~160 Ma) heating pulse was of short duration. The regional consistency of the data presented here, which is in contrast to many other thermochronometers in the IVZ, demonstrates the value of the rutile U–Pb technique for probing the thermal evolution of high-grade metamorphic terrains. In the IVZ, a significant decoupling between Zr-in-rutile temperatures and U–Pb ages of rutile is observed, with the two systems recording events ~120 Ma apart.

Keywords Ivrea–Verbano Zone · Rutile · U–Pb dating · Adriatic margin · Thermochronology

Communicated by Jochen Hoefs.

Electronic supplementary material The online version of this article (doi:10.1007/s00410-015-1135-6) contains supplementary material, which is available to authorized users.

✉ Tanya A. Ewing
tanya.ewing@unil.ch

[1] Research School of Earth Sciences, Australian National University, Canberra, ACT 0200, Australia

[2] Present Address: Institute of Earth Sciences, University of Lausanne, 1015 Lausanne, Switzerland

[3] Dipartimento di Scienze della Terra, Università di Torino, Via Valperga Caluso 35, 10125 Turin, Italy

Introduction

The European Alps represent a key locality to study the process of rifting leading to continental break-up, as different parts of both margins associated with the Jurassic continental rifting that led to the opening of the Tethys have been exposed by the Cretaceous–Tertiary Alpine orogeny (see Mohn et al. 2010 for a recent review). Within this context, the Ivrea–Verbano Zone (IVZ, Southern Alps, Italy) exposes a remarkably complete section through the

pre-rifting (Permian) lower crust of the Adriatic plate. In contrast to the parts of the Adriatic margin to the west, which underwent pervasive metamorphic overprinting during the Alpine orogeny (Beltrando et al. 2014), the IVZ has suffered little overprint from the Alpine orogeny. The IVZ is thus a prime locality to study the thermal history of the lower crust associated with Jurassic rifting and, ultimately, the onset of seafloor spreading. In spite of decades of study of the IVZ, its cooling history following the Paleozoic thermal peak remains relatively poorly known. Interpretation of the post-peak cooling history of the IVZ has been complicated by complex and sometimes contradictory geochronological data for many thermochronometers.

Rutile (TiO_2) is the high-pressure, high-temperature Ti phase (Ernst and Liu 1998; Liu et al. 1996) and occurs as an accessory mineral in a range of lower crustal lithologies, often as part of the peak metamorphic assemblage. Rutile has been shown to be capable of robustly preserving Zr-in-rutile temperatures from granulite facies or ultra-high-temperature conditions (e.g. Baldwin and Brown 2008; Ewing et al. 2013; Kooijman et al. 2012; Luvizotto and Zack 2009), but the U–Pb system in rutile is expected to record cooling through significantly lower temperatures of 500–650 °C (Cherniak 2000; Kooijman et al. 2010; Vry and Baker 2006). The common occurrence of rutile in some lower crustal lithologies combined with its moderate closure temperature for Pb make U–Pb geochronology of rutile ideally placed to investigate the post-peak thermal evolution of the lower crust during cooling and exhumation.

U–Pb dating of rutile from samples from throughout the IVZ has the potential to help resolve some of the inconsistencies observed in other geochronological datasets for this classic lower crustal section. Many metapelites from the IVZ contain rutile, which formed under peak metamorphic conditions in the Permian, and have high Zr-in-rutile temperatures that demonstrate that no retrogressive recrystallisation of rutile has occurred at temperatures below 750–800 °C (Ewing et al. 2013). Given that the closure temperature of Pb in rutile is significantly lower than the temperature of the last recrystallisation of rutile, U–Pb ages for this mineral are expected to universally record cooling through this closure temperature in all samples. U–Pb dating of rutile should therefore yield a dataset uncomplicated by effects such as growth or recrystallisation below the closure temperature, which could give ages relating to a range of different temperatures. Two previous studies have obtained U–Pb ages for rutile from the IVZ (Smye and Stockli 2014; Zack et al. 2011), but the three samples dated in these studies all came from within a small area in a single valley (Val d'Ossola). U–Pb dating of rutile from widespread samples from throughout the IVZ is required to assess the behaviour of this thermochronometer on the regional scale and facilitate comparison with ages obtained from other systems.

In this contribution, we present SHRIMP U–Pb ages for rutile from a suite of seven granulite facies metapelites from throughout the base of the IVZ lower crustal section, sampled across ~35 km along strike of the Paleozoic structural grain. We demonstrate that these rutile U–Pb ages record cooling on a regional scale, probably following episodic reheating, and examine the implications for the post-peak thermal history of this classic lower crustal section.

Fig. 1 Geological map of the central and northern IVZ. Modified after Barboza and Bergantz (2000), Siegesmund et al. (2008, after Handy et al. 1999) and with reference to Sinigoi et al. (1996), Boriani and Burlini (1995), Rutter et al. (2007), Mayer et al. (2000), Quick et al. (2003), Stähle et al. (2001) and Ewing et al. (2013). Samples analysed in this study are marked by stars. Isograds were originally mapped by Zingg (1980). The opx-in isograd marks the first appearance of orthopyroxene in mafic rocks and delineates the transition from amphibolite to granulite facies (Barboza and Bergantz 2000). *Green hexagon* shows the location of the sample from which rutile was U–Pb dated by Zack et al. (2011). *Green squares* indicate Smye and Stockli's (2014) samples for rutile U–Pb dating

Geological setting

The Ivrea–Verbano Zone (IVZ) in north-west Italy preserves a nearly uninterrupted section through the Permian lower continental crust, subsequently tilted by 90° to now be exposed in map view (e.g. Boriani et al. 1990; Demarchi et al. 1998; Handy et al. 1999; Quick et al. 1994; Sinigoi et al. 1996; Zingg et al. 1990; Fig. 1). To the north-west, the IVZ is separated from the Austro-Alpine and Penninic domains of the Western and Central Alps by the Insubric Line, which mainly preserves evidence of a multistage Alpine evolution starting from the Oligocene (Schmid et al. 1987). To the south-east, the IVZ is juxtaposed against the Strona-Ceneri Zone by a composite tectonic lineament made up of the Permian Cossato–Mergozzo–Brissago (CMB) line and the Jurassic Pogallo shear zone (Boriani et al. 1990; Handy 1987; Mulch et al. 2002a, b). The timing of tilting of the IVZ section to its current orientation is debated. It has been alternatively suggested that the tilting was largely achieved by the end of the Paleozoic (Boriani and Giobbi 2004), as a combined effect of Tethyan rifting and Alpine tectonics (Handy et al. 1999; Wolff et al. 2012), or mostly due to Alpine tectonics (e.g. Quick et al. 2009).

The IVZ is traditionally subdivided into two major units, the Kinzigite Formation and the Mafic Complex (Fig. 1). The Kinzigite Formation is dominated by amphibolite to granulite facies metapelites, with subordinate metagreywackes, metabasites, impure marbles and calc-silicate paragneiss (Henk et al. 1997; Quick et al.

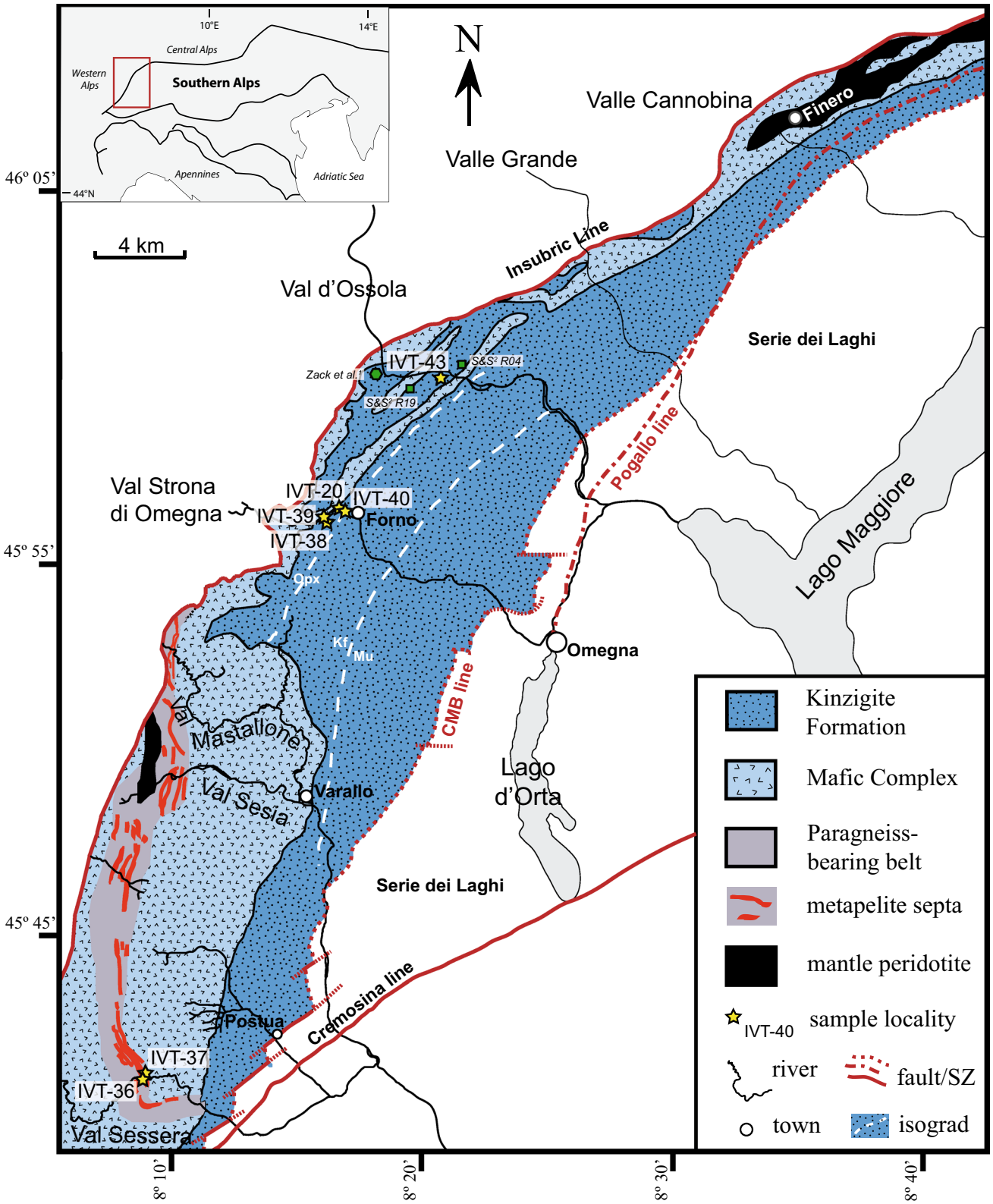

2003; Redler et al. 2013; Sills and Tarney 1984). Rutile is an accessory mineral in many granulite facies IVZ metapelites, where it formed during high-temperature metamorphism as part of the same reaction that produced garnet and partial melt (Ewing et al. 2013; Luvizotto and Zack 2009; Schnetger 1994).

The Mafic Complex is a dominantly gabbroic, noritic and dioritic intrusive complex up to 10 km thick that was emplaced into the Kinzigite Formation (Barboza and Bergantz 2000; Sinigoi et al. 1991; Voshage et al. 1990). Highly elongate slivers of metapelite derived from the Kinzigite Formation and referred to as "septa" have been incorporated within the Mafic Complex and are concentrated in the 1–2 km wide "paragneiss–bearing belt" (Sinigoi et al. 1994, 1996; Fig. 1).

Metamorphic grade in the Kinzigite Formation increases steadily from amphibolite facies in the south-east to granulite facies in the north-west, which was at the base of the lower crustal section in the Permian (Zingg 1980). Quantitative phase equilibria modelling for the Kinzigite Formation in Val Strona gave P–T conditions ranging from 3.5–6.5 kbar and 650–730 °C at amphibolite facies, to 10–12 kbar and 900–950 °C at granulite facies (Redler et al. 2012). Zirconium-in-rutile thermometry gave similar temperatures for granulite facies metapelites from the base of the Kinzigite Formation (900–930 °C), and higher temperatures for narrow (≤1 m) septa directly incorporated within the Mafic Complex (1000–1020 °C; Ewing et al. 2013).

The regional metamorphism responsible for the establishment of the amphibolite–granulite facies isograds occurred at 316 ± 3 Ma, as constrained by U–Pb geochronology of zircon (Ewing et al. 2013). The emplacement of the Mafic Complex generated a second episode of high-temperature metamorphism and anatexis during decompression, which affected only a 1–2-km aureole around the Mafic Complex (Barboza and Bergantz 2000; Barboza et al. 1999; Redler et al. 2012). Emplacement of the Mafic Complex culminated at 288 ± 4 Ma, as determined by U–Pb dating of zircon (Peressini et al. 2007), although the onset of the main igneous phase was probably as early as ~295 Ma (Sinigoi et al. 2011). Ongoing, but volumetrically minor, episodic magmatic activity affected both the lower and upper crust between 316 and 295 Ma, as demonstrated by recent zircon U–Pb dating of a range of small intrusive bodies in the Ivrea–Verbano and Strona–Ceneri Zones (Klötzli et al. 2014). Zircons from both metapelites and Mafic Complex magmatic rocks have revealed considerable complexity in U–Pb age spectra, with multiple events of metamorphic growth, recrystallisation and resetting in the Permian and Triassic (Ewing et al. 2013; Peressini et al. 2007; Vavra et al. 1996, 1999).

The post-Permian evolution of the IVZ includes multiple stages of relatively minor magmatic activity, mostly confined to the northernmost IVZ (Finero area). Despite the first-order similarities with the rest of the IVZ, a distinct Mesozoic evolution has been proposed for the northern part of the IVZ, based on (1) petrological differences from the central IVZ for the Mafic Complex, (2) the pervasive metasomatism experienced by the mantle bodies near the base of the Mafic Complex that is observed only in the Finero area, and (3) a Triassic (232 ± 3 Ma) intrusion age inferred for the Mafic Complex in the Finero area based on U–Pb geochronology of a sub-population of zircons (Mazzucchelli et al. 2010; Zanetti et al. 2013). The high-temperature Anzola shear zone (Val Grande–Val d'Ossola; Brodie et al. 1989; Brodie and Rutter 1987) has been speculatively suggested as a rift-related tectonic boundary between the northern (Finero) and central IVZ (Mazzucchelli et al. 2010; Zanetti et al. 2013).

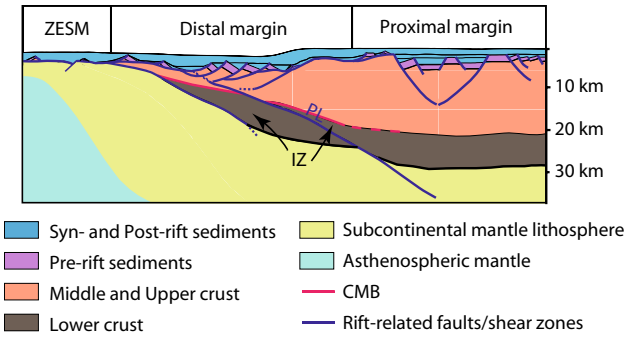

Fig. 2 Simplified paleogeographic section across the Adriatic margin after complete excision of the continental crust, in the Middle Jurassic. This section, which is modified after Handy et al. (1999) and Mohn et al. (2012), accounts for the field relationships between Ivrea-Verbano Zone (IVZ), Serie dei Laghi, Cossato-Mergozzo-Brissago Line (CMB) and Pogallo Line (PL) observed between the Cannobina Valley and the Sessera Valley. *ZESM* zone of exhumed subcontinental mantle

Episodic Triassic to Jurassic mantle-derived magmatism in the northernmost IVZ is recorded by alkaline dikes and pegmatoids intruding the Finero peridotite, with zircon U–Pb ages ranging between ~190 and 225 ± 13 Ma for these localised intrusions (Schaltegger et al. 2015; Stähle et al. 1990). Associated Late Triassic metasomatic events are also recorded in this area. Apatite-rich peridotite layers in the Finero phlogopite have been interpreted as metasomatic in origin and apatite U–Pb dated at 215 ± 35 Ma (Morishita et al. 2008). Chromitites within the Finero phlogopite peridotite have also been attributed a metasomatic origin, the timing of which is constrained by a 208 ± 2 Ma upper intercept zircon U–Pb age (Grieco et al. 2001). Mantle-derived magmatism is also recorded in the southernmost IVZ (near the town of Baldissero, ~40 km south-west of Fig. 1) by 204 ± 31 Ma to 198 ± 29 Ma intrusion ages of mantle-derived dikes determined by Sm–Nd isochrons (Mazzucchelli et al. 2010). Subsequent to this period of episodic magmatism and metasomatism, rifting resulted in regional exhumation of sub-continental mantle to the floor of the Alpine Tethys at 167–160 Ma (e.g. Bill et al. 2001; Chiari et al. 2000), when the IVZ was located at the

transition between the proximal and distal Adriatic margin (Beltrando et al. 2014; Mohn et al. 2010; Fig. 2).

Thermochronology of the IVZ

Two previous studies have presented U–Pb ages for rutile from the IVZ. Smye and Stockli (2014) used depth profiling by laser ablation split stream ICP-MS to measure U–Pb age profiles in the outermost ~30 µm of rutiles from two granulite facies metapelites from Val d'Ossola. They obtained dates of 140–190 Ma for individual depth slices, with dates plateauing at 180–190 Ma after ~15 µm. Zack et al. (2011) obtained an age of 181 ± 4 Ma for the largest rutiles from one sample from Val d'Ossola.

A wealth of geochronological data from other thermochronometers that record temperatures of 300 to ≥ 600 °C exists for the IVZ (Fig. 7). These data are relevant for comparison with rutile U–Pb ages and will be briefly reviewed here. The largest available dataset for a single thermochronometer within the IVZ comes from Ar–Ar dating of amphibole, but many of these data are contradictory. In a transect through the IVZ in Val Strona, Siegesmund et al. (2008) obtained ^{40}Ar–^{39}Ar hornblende ages that show a marked east–west gradient, decreasing from 257 ± 1 Ma at the CMB line to 202 ± 13 Ma at the Insubric line. These ages are in conflict with the older ^{40}Ar–^{39}Ar hornblende ages of Boriani and Villa (1997) for three samples from Val Strona, which showed no systematic east–west change. With the aid of chemical correlation diagrams, Boriani and Villa (1997) proposed ages of 280–240 Ma and <220 Ma for two distinctive amphibole generations observed in thin section in these samples. Brodie et al. (1989) obtained a minimum ^{40}Ar–^{39}Ar age of 247 ± 7 Ma for hornblende from an undeformed gabbro in Val d'Ossola, and hornblende ^{40}Ar–^{39}Ar ages of 215 ± 5 Ma and 210 ± 5 Ma for a metagabbro from an immediately adjacent high-temperature shear zone (Anzola–Forno shear zone; Rutter et al. 2007). This age difference was ascribed to reduced Ar retention in finer-grained syn-kinematic amphibole with respect to the coarser hornblende in the wall rock gabbro, in the context of post-Permian, post-kinematic conductive cooling (Brodie et al. 1989). An alternative interpretation would be that the younger ages record Late Triassic deformation-induced recrystallisation, rather than diffusive loss of Ar. This interpretation would be consistent with the observation that meta-mafic rocks further to the west of the Anzola–Forno shear zone in Val Strona yielded Permian to Triassic ^{40}Ar–^{39}Ar apparent ages (Boriani and Villa 1997). As already suggested by Boriani and Villa (1997), it appears that ^{40}Ar–^{39}Ar ages of amphiboles in the Ivrea Zone are not controlled only by diffusive loss of Ar and that recrystallisation of hornblende also plays an important role. This observation indicates that caution is required in using ^{40}Ar–^{39}Ar hornblende ages to infer the post-Permian thermal evolution of the IVZ based on an inferred closure temperature (calculated as ≥550 °C for hornblende from the IVZ by Siegesmund et al. 2008). Caution is also demanded by the considerable excess Ar observed in many ^{40}Ar–^{39}Ar analyses of IVZ hornblendes (Siegesmund et al. 2008), while mixed age populations (e.g. Boriani and Villa 1997) present a further complication.

Ar–Ar dating of muscovite in a sample from the Pogallo line north of Val d'Ossola yielded a plateau Ar–Ar muscovite age of 182.0 ± 1.6 Ma (Mulch et al. 2002a). This result was interpreted to indicate that shearing at upper greenschist facies conditions along this shear zone took place in the Lower Jurassic (Mulch et al. 2002a). Siegesmund et al. (2008) obtained K–Ar ages for biotite along the Val Strona transect, which decreased steadily towards deeper parts of the section from 228 ± 5 Ma at the CMB line to 156 ± 3 Ma at the Insubric line. Wolff et al. (2012) presented biotite K–Ar ages for three samples from Val d'Ossola and the northernmost IVZ, which ranged from 163 ± 3 Ma and 184 ± 13 Ma, younger for a given NW–SE position than Siegesmund et al.'s (2008) K–Ar biotite ages in Val Strona to the south. K–Ar ages should, however, be treated with caution, as this technique does not allow testing of whether the dated mineral separate contains more than one mica generation, effectively resulting in mixed ages. Nor does it allow the identification of excess Ar, which if present would lead to erroneously old ages.

Our rutile-bearing metapelites span much of the length of the IVZ, but a relatively narrow NW–SE range (Fig. 1). Units dated by other techniques that come from equivalent positions to our samples yielded Ar–Ar hornblende ages of ~210 Ma according to Siegesmund et al. (2008) or ~240 Ma according to Boriani and Villa (1997), and K–Ar biotite ages of 160–170 Ma in Val Strona and Val d'Ossola (Siegesmund et al. 2008; Wolff et al. 2012). Our sample from Val d'Ossola (IVT-43) was collected between ~1 and 3 km from each of the three samples dated with rutile U–Pb geochronology by Smye and Stockli (2014) and Zack et al. (2011).

Samples

Rutile from seven granulite facies metapelite samples was U–Pb dated (Fig. 1, Table 1). The samples come from three valleys within the IVZ: Val d'Ossola (central–northern IVZ), Val Strona di Omegna (central IVZ), and Val Sessera (southern IVZ), and spread across ~35 km along the base of the IVZ. Granulite facies metapelites comprise layers of restite (Grt + Qz + Sil ± Kfs ± Rt) and leucosome (Grt + Qz + Kfs + Pl ± Rt), generally interlayered on a centimetre scale (Table 1; mineral abbreviations after

Table 1 Summary of characteristics of IVZ metapelite samples analysed in this study

Sample	ANU #	Lithology	Grid reference		Mineral assemblage		Peak $T_{Zr\text{-}in\text{-}Rt}$ (°C)^	Zrn U–Pb ages (Ma)^
			E	N	Major	Accessory		
Val d'Ossola								
IVT-43	09-020	Layered metapelite restite and leucosome	449091	50 92841	Grt + Qtz + Kfs + Pl + Sil	Rt	900 ± 40[a1]	
Val Strona								
IVT-40	09-018	Garnetiferous leucosome	444335	50 87453	Grt + Qtz + Kfs + Pl	Rt + Zrn	910 ± 40[a2]	
IVT-20	09-009	Garnetiferous leucosome	443955	50 87588	Grt + Qtz + Kfs + Pl	Rt + Bt + Zrn	910 ± 40[a2]	316 ± 3, 276 ± 4, 258 ± 3
IVT-38	09-016	Layered metapelite restite and leucosome	443502	50 86983	Grt + Qtz + Pl + Kfs + Sil	Bt + Rt	910 ± 40	
IVT-39	09-017	Layered metapelite restite and leucosome	443247	50 86989	Grt + Kfs + Pl + Sil	Rt + Bt	910 ± 40	
Val Sessera								
IVT-36	09-014	Layered metapelite restite and leucosome	433957	50 60990	Gt + Qtz + Kfs + Sil	Rt	930 ± 40	
IVT-37	09-015	Metapelitic restite	433897	50 61018	Gt + Qtz + Sil + Kfs	Rt	920 ± 40	

Grid references are given as UTM coordinates relative to the WGS84 datum. ^ Ewing et al. (2013). [a] Peak temperature not recorded in this sample, inferred from adjacent samples [1] IVT-42 and [2] IVT-38 + IVT-39

Whitney and Evans 2010). The samples are made up of interlayered restite and leucosome, except for IVT-20 and IVT-40 (leucosome only) and IVT-37 (purely restitic). Samples from Val d'Ossola and Val Strona come from the granulite facies part of the Kinzigite Formation. The Val d'Ossola samples come from ~800 m west of the Anzola high-temperature shear zone (after Brodie et al. 1989; Brodie and Rutter 1987). The two samples from Val Sessera come from one particularly thick septum within the Mafic Complex (Fig. 1). Characteristics of samples analysed in this study are summarised in Table 1. More detailed descriptions of all samples, as well as rutile trace element and Zr thermometry data, were presented by Ewing et al. (2013), who also reported U–Pb ages of zircons from selected samples. Hafnium isotope analyses of rutiles from the same samples were presented by Ewing et al. (2014).

Methodology

Samples were crushed to <420 μm, and rutile grains separated using standard heavy liquid and magnetic techniques. Rutiles were hand-picked and mounted in 2.5 cm epoxy discs, which were polished to expose the mid-sections of grains. Care was taken to mount rutiles of broadly similar grainsize in each mount, with separate mounts being made in the case of significant differences in grainsize, so that the exposed sections of each grain are as close as possible to true mid-sections. Rutiles were photographed in reflected and transmitted light using a standard petrographic microscope, and backscattered electron (BSE) imaged on a Cambridge S360 scanning electron microscope at the Australian National University Centre for Advanced Microscopy, with operating conditions of 15 kV accelerating voltage, 3 nA current, and a working distance of 15–18 mm.

U–Pb ages of rutiles were determined by sensitive high-resolution ion microprobe (SHRIMP) in five sessions on SHRIMPs II and RG at the Australian National University. Instrumental set-up and data treatment follow Williams (1998) and are the same as for zircon except for the differences outlined below. Because of the relatively low U content of rutile, an unfiltered primary oxygen beam was used to maximise output of secondary ions. This produced much larger primary ion currents (5–30 nA, but usually >10 nA) than the mass-filtered O_2 beam used for zircon analyses. Each analysis comprised six scans through ten masses, with the addition of $^{270}UO_2^+$ to the usual zircon run table, and longer count times for some isotopes (Table 2). A peak at ~195.96 AMU was used as a reference peak for calculation of absolute U and Th concentrations and for peak-centering after the large magnet jump from high masses. The magnitude of this reference peak was observed to vary by up to a factor of two between rutiles. U and Th contents

Table 2 Typical run table for SHRIMP U–Pb analysis of rutile

Mass station	Isotope	Approx. mass (AMU)	Count time (s)
1	Reference	195.96	2
2	^{204}Pb	203.99	10
3	Background	204.04	10
4	^{206}Pb	205.99	25–30
5	^{207}Pb	206.99	30
6	^{208}Pb	208.00	10
7	^{238}U	238.08	15–20
8	^{248}ThO	248.08	2–5
9	^{254}UO	254.10	2–3
10	$^{270}UO_2$	270.11	2

Count times are for one scan; six scans are collected per analysis. *AMU* atomic mass units

calculated from SHRIMP analyses are therefore only accurate to within a factor of two. We did not observe a stable, reproducible peak at ~192 AMU as used by Taylor et al. (2012) for a reference.

Data were processed with SQUID 1.13a (Ludwig 2001) using the same ln(Pb*/U)/ln(UO/U) calibration as for zircon (e.g. Williams 1998). Because of the higher count rates on UO and UO_2 relative to U, some previous SHRIMP studies have used alternative calibrations for rutile: ln(Pb*/UO)–ln(U/UO) (Clark et al. 2000) and ln(Pb/U)–ln(UO_2/UO) (Taylor et al. 2012). However, in our sessions, the traditional ln(Pb*/U)/ln(UO/U) calibration performed at least as well as alternative calibrations for rutile, and sometimes better.

A common Pb correction was applied to all rutile U–Pb data, using a ^{207}Pb correction (Williams 1998). Rutile analyses are typically corrected for common Pb with a ^{208}Pb correction, taking advantage of the incompatibility of Th in rutile (e.g. Brenan et al. 1994; Foley et al. 2000) and thus the near absence of radiogenic ^{208}Pb in rutile (Zack et al. 2011). However, for many of our IVZ rutiles, the errors calculated by SQUID 1.13a for ^{208}Pb-corrected ^{206}Pb/^{238}U ages were extremely large, and up to seven times higher than those for the ^{207}Pb-corrected age for the same analysis. The ^{207}Pb- and ^{208}Pb-corrected ages were always indistinguishable, so we use a ^{207}Pb correction for common Pb, which gives more reasonable errors that are consistent between analyses. An interference on ^{204}Pb was observed for some rutile samples, making a ^{204}Pb common Pb correction inappropriate for SHRIMP analyses of rutile. The Broken Hill Pb composition is a good approximation of surface Pb contamination in our laboratory and was used for correction of the standard. An age-dependent model common Pb composition (Stacey and Kramers 1975) was used for unknowns.

Our in-house *Wodgina* rutile standard was used for Pb–U calibration of rutile analyses (Ewing 2011). The Wodgina standard is a chip from a rutile megacryst from a locality of the same name in north-western Australia, which was obtained from the Western Australian Museum. Four chips of Wodgina rutile gave a concordant TIMS U–Pb age of 2845.4 ± 0.5 Ma, excluding decay constant uncertainties (Ewing 2011). In our SHRIMP sessions, this standard gave 3.5–5.5 % calibration errors (2σ), with rejection of a few reversely discordant analyses in most sessions due to analytical artefacts (Ewing 2011; Table S1). Analyses to be rejected were independently identified on a plot of UO/U versus UO_2/U, referred to as the "3-U plot". It has been observed in zircon sessions over many years that on the 3-U plot all well-behaved analyses of standards and unknowns alike, irrespective of age, fall on a single trend,

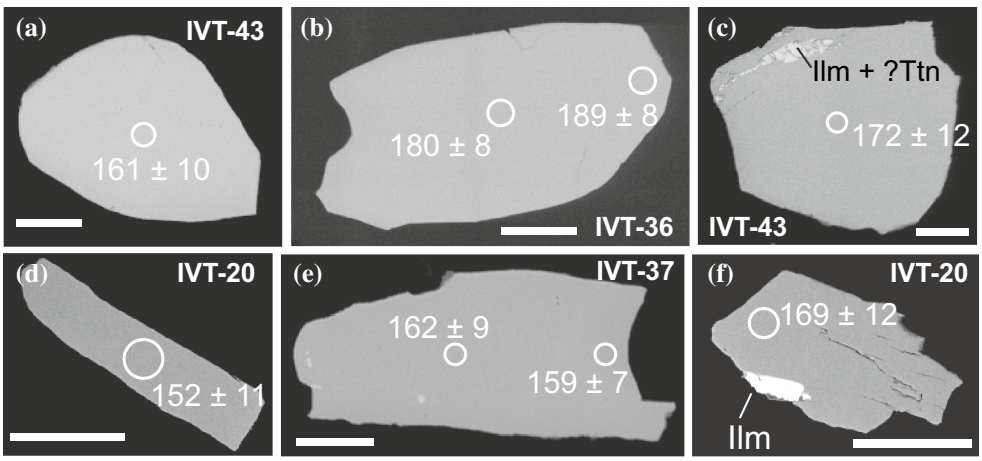

Fig. 3 Representative backscattered electron (BSE) images of rutiles from IVZ metapelites, showing (**a**, **b**, **d**, **e**) typical unzoned rutiles and (**c**, **f**) rutiles with partial replacement by ilmenite ± other phases. Scale bars are 100 μm. White circles mark SHRIMP spots, with dates given at the 2σ level

with any outliers giving unreliable ages (I.S. Williams, pers comm). UO/U and UO_2/U ratios for the 3-U plot were calculated with the PRAWN data reduction program written by T.R. Ireland.

Although the Wodgina rutile was originally a megacryst, prior to analysis, it was broken into many smaller pieces comparable in size to rutiles from the IVZ samples. Three to nine chips of Wodgina mounted in random orientations were analysed in all sessions, with six to nine chips in all but one session. This ensures that a range of crystallographic orientations were analysed for the standard as for unknowns, which can be important to avoid orientation-related effects in SHRIMP U–Pb analysis of rutile (Taylor et al. 2012).

U–Pb data are presented on Tera-Wasserburg diagrams with 2σ error ellipses and uncorrected for common Pb to allow visualisation of the proportion of common Pb affecting analyses, noting that it is not possible to plot analyses ^{207}Pb-corrected for common Pb on concordia diagrams. Ages presented in other diagrams (e.g. probability density functions) and given in the text are always ^{207}Pb-corrected for common Pb. IsoPlot Ex 3.5 (Ludwig 2003) was used to produce Tera-Wasserburg concordia diagrams (Tera and Wasserburg 1972) and to calculate weighted means. Individual dates are quoted with 1σ errors, while ages of populations are quoted at the 95 % confidence level.

Results

Rutile grains from the dated samples are generally homogeneous in BSE images, with no indication of zoning or preservation of more than one generation of rutile (Fig. 3a, b, d, e). Partial replacement of rutile by either blobs or needles of ilmenite, or arcuate areas made up of a mixture of phases including ilmenite, is common and easily identified in BSE images and avoided during analysis (Fig. 3c, f). The dated samples have rutile with average U contents determined by LA-ICPMS of 10–50 ppm (from data of Ewing et al. 2013).

All dated rutile grains contain negligible Th, with Th/U measured by SHRIMP always <0.009 and usually <0.0002. The 137 analyses of rutile have common Pb contents ranging from 0.6 to 86 % common ^{206}Pb ($^{206}Pb_c$; Fig. 4, Table S1), with an average of 7 % after rejection of six high common Pb analyses. All ^{206}Pb/^{238}U ages referred to in the text and used in calculation of population ages are common Pb corrected. Two analyses with significantly older ^{206}Pb/^{238}U ages were rejected on the basis of being outliers on the 3-U plot. One substantially younger (~140 Ma) analysis from IVT-37 was rejected solely because it was an outlier in terms of ^{206}Pb/^{238}U age (Fig. 4).

Fig. 4 Tera–Wasserburg concordia diagrams for IVZ rutile samples, uncorrected for common Pb. Error ellipses are 2σ. Excluded analyses are shown in *light grey* with a *solid border* (high common Pb) or dashed border (^{206}Pb/^{238}U outlier)

^{206}Pb/^{238}U dates for IVT-38 define two major distinct peaks on a probability density plot (Fig. 5d) and have a cumulative MSWD of 14 that indicates more than one age population is present. No independent criteria (such as grainsize or trace element chemistry) have been found to divide the IVT-38 dates into two populations but Isoplot's unmix ages function gives ages of 164 ± 3 Ma and 140 ± 2 Ma (2σ) for this sample. For the other six samples, probability density functions of individual U–Pb dates do not show more than one completely distinguished age population (Fig. 5). However, all of these probability density functions, each of which has 15–38 ^{206}Pb/^{238}U dates, deviate noticeably from simple Gaussian curves, frequently showing a subordinate inflection or broad tailing towards older dates up to 180–200 Ma (Fig. 5a–g). The six samples apart from IVT-38 have MSWDs between 2.9 and 6.8, indicating significant scatter that cannot be explained only by the analytical errors.

There is no relationship resolved between ^{206}Pb/^{238}U dates and effective diffusion radius (i.e. the shortest distance to the edge of the rutile grain) for any sample (Fig. 6a, Fig. S1). For fourteen large rutiles from five samples, analyses were performed near both core and rim of the rutile, but a difference in age was never resolved for these core–rim pairs with the exception of one rutile from IVT-38 that gave dates of 180 ± 4 Ma in the core and 145 ± 4 Ma at the rim (Fig. 6b). Some, but not all, of the dated rutiles show evidence of exsolution needles of ilmenite, which are a common feature of rutile that could potentially modify its effective diffusion radius. No relationship was observed between measured U–Pb dates and the presence or absence of ilmenite exsolution needles in BSE images. However, we cannot exclude the presence in some rutiles of ilmenite lamellae that are not exposed at the surface and thus not detected in BSE images. We therefore cannot rule out the possibility that fast diffusion pathways created by ilmenite needles—or other undetected defects such as subgrain boundaries—played a role in the diffusion behaviour of Pb in some rutiles. LA-ICPMS trace element data exist for around half of the rutiles U–Pb dated (in Ewing et al. 2013). There is no correlation between U–Pb dates and concentration of trace elements including U, Pb, Si, Zr, Hf, Nb, Ta, Cr, V and Fe for these rutiles (e.g. Fig. S2a–c). The analysed rutiles fall into two distinct groups in terms of Zr-in-rutile temperature, at 900–950 and 750–800 °C, respectively, but both groups give the full range of U–Pb dates (160–180 Ma; Fig. S2d).

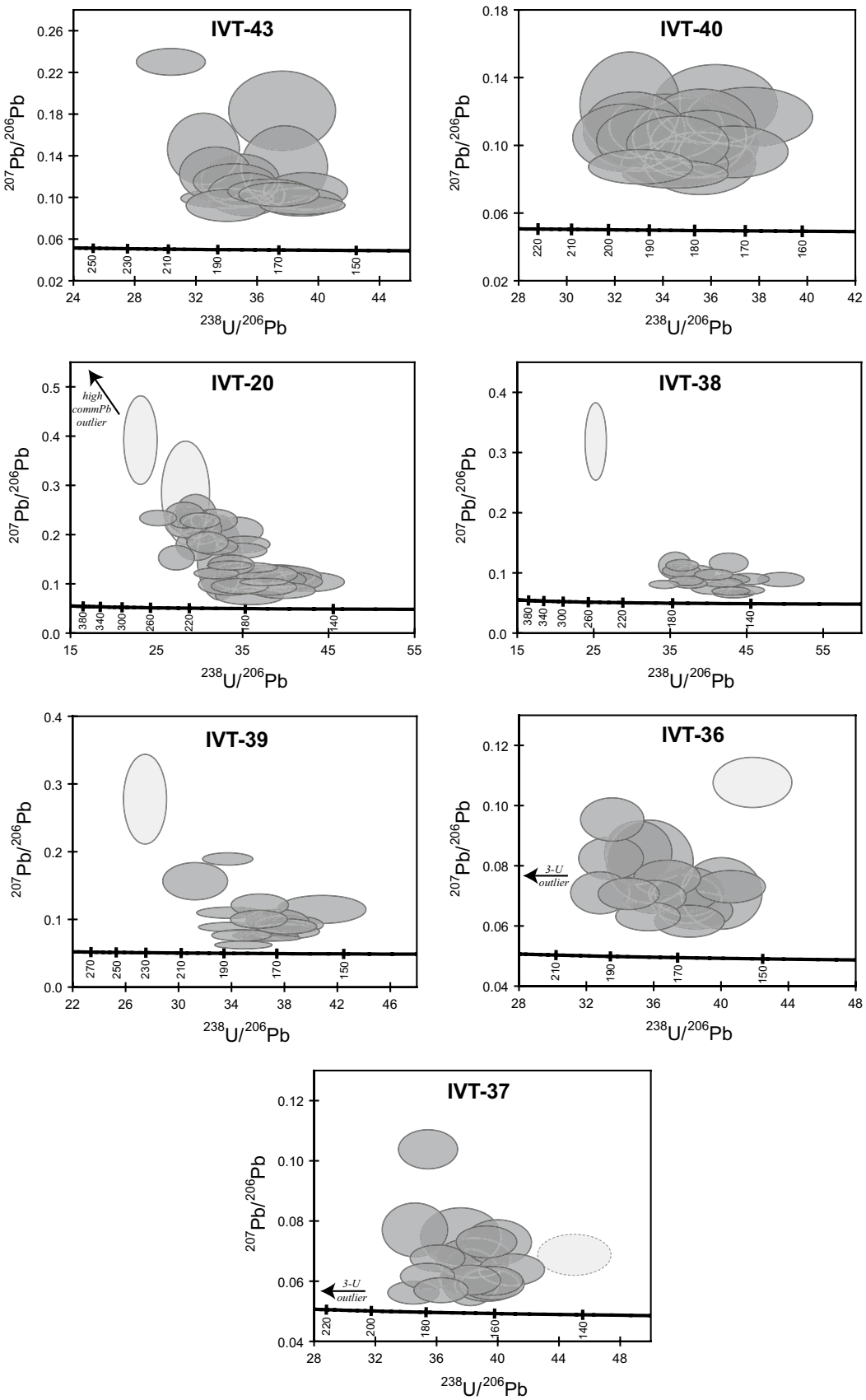
IVT-43
IVT-40
IVT-20
high commPb outlier
IVT-38
IVT-39
IVT-36
3-U outlier
IVT-37
3-U outlier
$^{207}Pb/^{206}Pb$
$^{238}U/^{206}Pb$

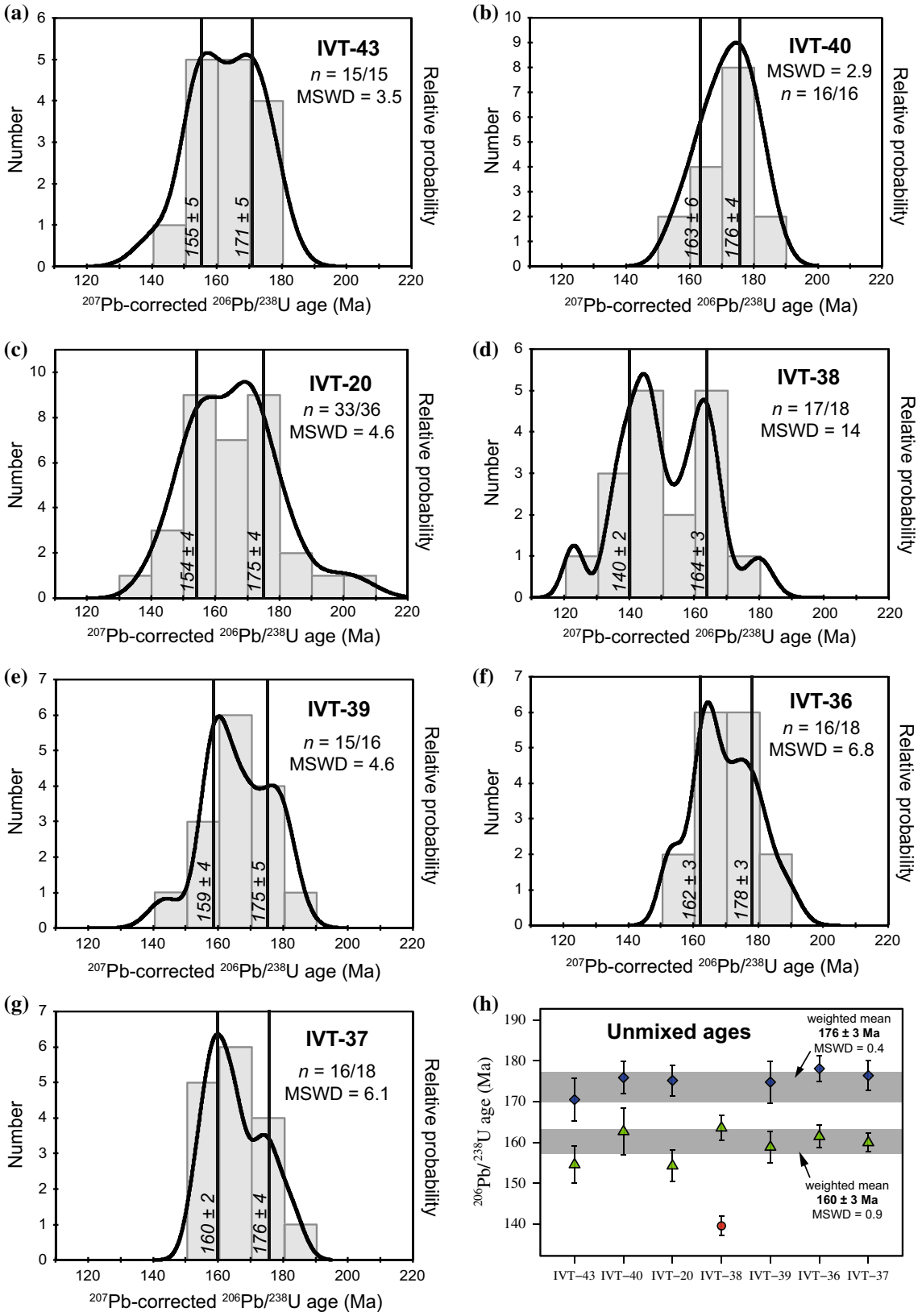

The non-Gaussian probability density functions of U–Pb dates from each sample suggest that there is age complexity that cannot be fully distinguished at the level of precision obtained for these relatively low-U rutiles. Qualitatively, the probability density functions suggest that most or all samples record a main age population at ~160 Ma and a

◀ **Fig. 5** **a–g** Probability density functions and histograms for ^{207}Pb-corrected ^{206}Pb/^{238}U ages of IVZ rutile samples. *Black vertical lines* show the ages (annotated with 2σ errors) obtained by the 'unmix ages' function of Isoplot (Ludwig 2003) and given in Table 3. Histogram bin size is equal to the median 2σ age error. Note that the calculation of the probability density function relies only on individual dates and their errors, and is completely independent of bin size. It is therefore more robust than the histogram, which also does not take account of the precision of individual analyses. Histograms are included only to illustrate the number of analyses. **h** Ages obtained for each sample from unmix ages. Weighted means of the older (diamond symbols) and younger (triangles) populations are shown as grey bands at the 95 % confidence level. The youngest population, observed only in IVT-38, is distinguished by a circle symbol. Errors on age populations are shown excluding the calibration error, but the propagated errors (Table 3) were used for calculation of weighted means

second, older age population that is not fully resolved at the precision of these analyses. This is supported by the high MSWDs of ^{207}Pb-corrected ^{206}Pb/^{238}U ages, which range between 3 and 6 and indicate that the data do not represent a single age population in any given sample. Given this complexity, simply taking a weighted mean of all analyses for a given sample is not justified, as this mean will be skewed by the subordinate older populations of ages. Instead, we used Isoplot Ex 3.5's unmix ages function to extract two age populations from ^{207}Pb-corrected ^{206}Pb/^{238}U age data for each sample (Table 3). The unmix ages function is based on the unmixing algorithm of Sambridge and Compston (1994), which is specifically designed to extract age populations that are not clearly distinguished from datasets such as ours in a robust, statistical way. The only inputs to this algorithm are the individual dates and their errors, and the number of populations to extract. The latter we set to two, as this is the number of partially resolved (major) populations suggested by the probability density functions of most samples. Using this function, we obtain two age populations of ~160 and ~175 Ma in most samples (Fig. 5h, Table 3). The only exception is IVT-38, which has the distinctly younger age population at 140 ± 2 Ma and a 164 ± 3 Ma population (Table 3). The calibration error of the relevant SHRIMP session(s) was propagated onto the error of each age population extracted from the samples by unmix ages (Table 3), and these expanded errors were used for calculation of weighted means. The weighted mean of the older populations extracted by unmix ages (six samples) gives an age of 176 ± 3 Ma (2σ), while the weighted mean of ~160 Ma populations (all samples) is 160 ± 3 Ma (Fig. 5h). Given the 3.5–5.5 % calibration errors for SHRIMP sessions, a more conservative estimate of precision may be appropriate for these pooled ages when the absolute age is important. Taking the precision to be 4.5 % gives regional ages of 160 ± 7 and 176 ± 8 Ma, noting that these expanded errors are important only for the absolute (not relative) ages, i.e. for the timing of the geological events these ages are interpreted to record and for comparison with other geochronological datasets. This error does not need to be taken into account to assess whether the two age populations are resolved from one another, which they are given that they do not overlap at the level of the 95 % confidence errors on the weighted means.

The 140 ± 2 Ma age population in IVT-38 is not recorded in any other sample, although isolated analyses of this age are occasionally observed (e.g. one excluded analysis in IVT-37; Fig. 4). The reason for the appearance of a ~140 Ma age population only in IVT-38 is unclear. IVT-38 is a sample of unretrogressed interlayered restite–leucosome, which was collected from approximately the same location as IVT-39 and within ~1.5 km of all Val Strona samples. It is one of the most pristine samples collected from the IVZ and is not mineralogically different from other restitic metapelites. The restricted occurrence of the ~140 Ma age group, as well as the fact it forms a discrete population in IVT-38 rather than a tailing of ages from the main ~165 Ma population, suggests localised resetting of U–Pb ages in some rutiles only. This would most easily be achieved by interaction with fluids. The 140 ± 2 Ma age does not correspond to any previously documented tectonometamorphic event in the IVZ.

Discussion

Closure temperature of Pb in rutile

Interpretation of rutile U–Pb ages hinges on knowledge of the temperature at which Pb diffusion ceases in rutile, locking in the U–Pb ratio. The closure temperature of Pb in rutile, here abbreviated to $T_{C\ (Pb–Rt)}$, has been the subject of debate for several decades.

The original estimate of $T_{C\ (Pb–Rt)}$ was 380–420 °C for slow cooling rates (0.5–1.0 °C/Ma) and rutiles with radii of 70–210 μm, determined using an empirical field calibration (Mezger et al. 1989). Experimental diffusion data gave conflicting results, with a much higher closure temperature of 580–630 °C for the same range of grainsizes and a similar cooling rate (Cherniak 2000). This higher closure temperature was subsequently corroborated by both a second empirical field calibration (Vry and Baker 2006), and diffusion profile modelling of Pb in rutile from natural samples (Kooijman et al. 2010). It is worth noting that all of these studies were conducted in terrains with similar slow cooling rates; $T_{C\ (Pb-Rt)}$ would be expected to be even higher in terrains with more rapid cooling rates. A T_C of Pb in rutile in excess of 620 °C, in agreement with experimental diffusion data, is also supported by the preservation of prograde ages (~33 Ma) in rutile from a metapelite

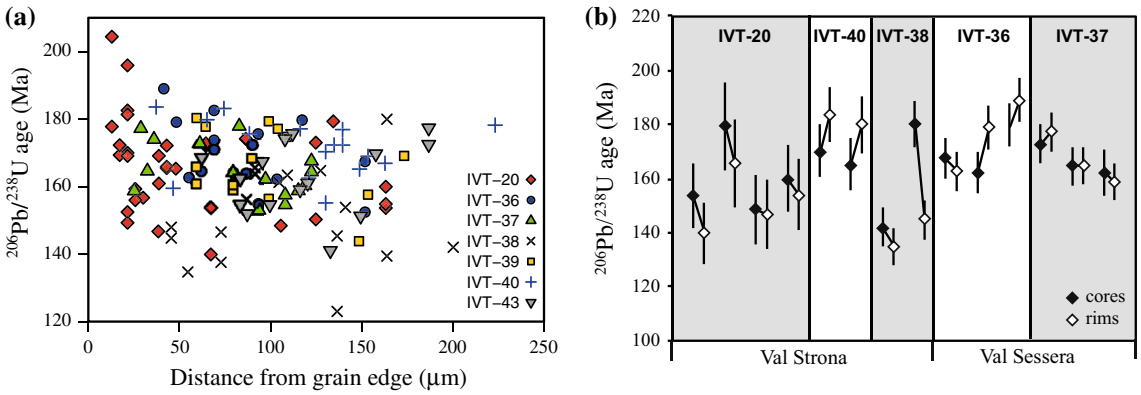

Fig. 6 **a** ^{207}Pb-corrected $^{206}Pb/^{238}U$ age versus distance from grain edge for IVZ rutile analyses. Error bars are omitted for clarity. Distance from the grain edge is taken as the shortest distance to the edge of the grain from the point of analysis, and is accurate to ± 10–20 µm. Separate plots for each sample including error bars on dates are plotted in Fig. S1. **b** $^{206}Pb/^{238}U$ dates (2σ) for cores and rims of the same rutiles. Core–rim pairs are joined by a line

Table 3 Output of Isoplot's 'unmix ages' function for IVZ rutile samples

Sample	Calib. error (2σ)	Older age population				Younger age population				Rel. misfit
		Age (Ma)	±2σ (Ma)	±2σ incl. calibration^	Proportion	Age (Ma)	±2σ (Ma)	±2σ incl. calibration^	Proportion	
IVT-43	4.5 %[a]	171	5	9	0.52	155	5	8	0.48	0.87
IVT-40	4.3 %	176	4	9	0.67	163	6	9	0.33	0.90
IVT-20	4.8 %[a]	175	4	9	0.53	154	4	8	0.47	0.84
IVT-38	3.3 %	164	3	6	0.47	140	2	5	0.53	0.55
IVT-39	4.5 %[a]	175	5	9	0.46	159	4	8	0.54	0.81
IVT-36	3.3 %	178	3	7	0.48	162	3	6	0.52	0.70
IVT-37	3.3 %	176	4	7	0.33	160	2	6	0.67	0.68

^2σ errors from unmix ages and SHRIMP calibration error for the relevant session(s) propagated in quadrature. [a] For samples analysed over two sessions, the average of the calibration errors was used for propagation

from the Barrovian sequence of the Central Alps, where peak temperatures of 620 °C were reached much later at 22 Ma (Boston et al. 2013). However, a higher closure temperature for Pb in rutile has not been universally accepted, with some workers arguing for a lower $T_{C\ (Pb\text{-}Rt)}$ based on the fact that U–Pb ages of rutile are generally similar to or slightly younger than U–Pb titanite and Ar–Ar hornblende ages for the same area (e.g. Blackburn et al. 2011; Li et al. 2003; Schmitz and Bowring 2003). It is noted that these studies presented TIMS (whole-grain) U–Pb ages of rutiles, which do not allow assessment of the development of diffusion-related age profiles within grains.

Empirical calibrations of closure temperature are based on the comparison of ages of the system of interest (in this case, U–Pb in rutile) to ages of other geochronometers with known closure temperatures. Since the pioneering study of Mezger et al. (1989), the closure temperatures of most of the geochronometers they used to calibrate the T_C of Pb in rutile have been revised substantially upwards (e.g. their calibration was based on a T_C of 600–700 °C for U–Pb in monazite and of 400–450 °C for Ar–Ar in hornblende). It is therefore no longer justified to use the $T_{C\ (Pb\text{–}Rt)}$ of 380–420 °C originally calculated by Mezger et al. (1989). Vry and Baker (2006) recalculated $T_{C\ (Pb\text{–}Rt)}$ directly from the data of Mezger et al. (1989) taking into account the subsequent upwards revision of the T_C of other systems and obtained a revised $T_{C\ (Pb\text{–}Rt)}$ of 500–540 °C. Taking this into account, no study provides evidence for a T_C of Pb in rutile lower than ~500 °C for geologically relevant cooling rates.

A minimum $T_{C\ (Pb\text{–}Rt)}$ of 500 °C is not contradicted by the observation that in many terranes Ar–Ar ages for hornblende are older than or overlap with rutile U–Pb ages. It is worth noting that the closure temperature of Ar–Ar in hornblende is not well constrained, with significant differences between estimates from hydrothermal experiments and field-based studies (e.g. Villa et al. 1996). Neither is a high closure temperature for Pb in rutile contradicted by the widespread observation of younger U–Pb ages for rutile

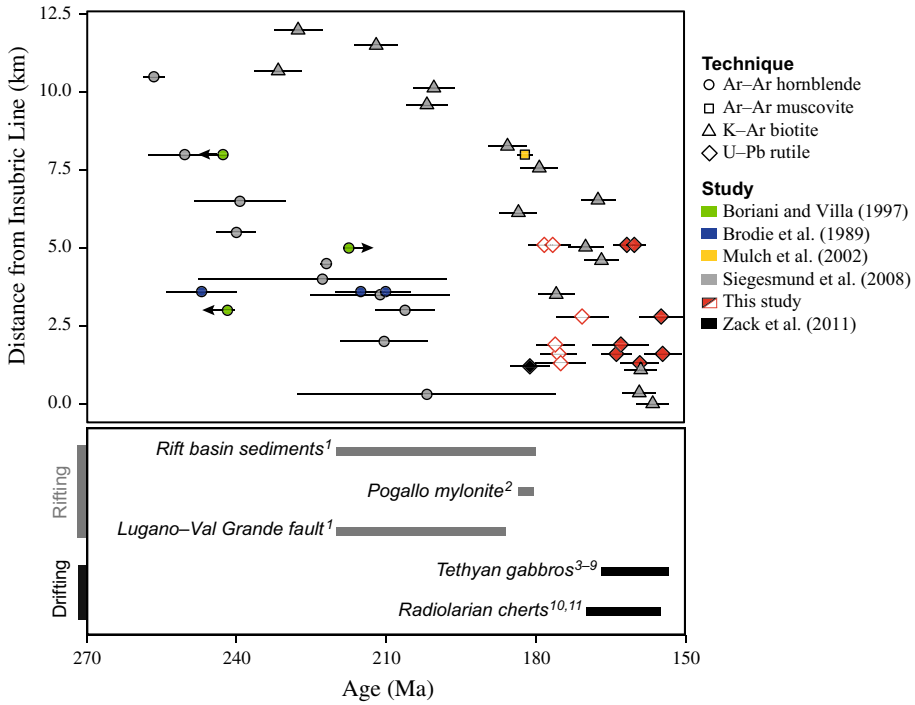

Fig. 7 *Upper* compilation of IVZ literature data for thermochronometers in the 300–600 °C range. Errors are 2σ or 95 % confidence. *Arrows* indicate minimum or maximum ages. Rutile U–Pb data from this study are shown for comparison, with the older and younger populations extracted by unmix ages distinguished for each sample. The ~140 Ma age population from IVT-38 is not shown. *Lower* age constraints from the literature for the Tethyan rifting and subsequent drifting phase throughout the Adriatic margin compiled from: [1] Bertotti et al. (1993), [2] Mulch et al. (2002a), [3] Bill et al. (1997), [4] Kaczmarek et al. (2008), [5] Li et al. (2013), [6] Liati et al. (2005), [7] Rubatto et al. (1998), [8] Rubatto and Scambelluri (2003), [9] Schaltegger et al. (2002), [10] Bill et al. (2001), and [11] Chiari et al. (2000)

than titanite in a given area (e.g. Corfu and Easton 2001; Flowers et al. 2006; Mezger et al. 1989). Experimental diffusion data for titanite give a closure temperature of ~575–700 °C for grain radii of 0.1–1.0 mm and cooling rates of 2–10 °C/Ma (Cherniak 1993). Field-based studies provide evidence for a T_C of Pb in titanite in excess of 660–700 °C, and even up to 750 °C, in at least some cases (Frost et al. 2001; Rubatto and Hermann 2001; Spencer et al. 2013).

For the range of effective diffusion radii analysed in this study (30–200 μm) and cooling rates of 2–10 °C/Ma, a closure temperature of 550–650 °C is calculated for rutile from the experimental diffusion data of Cherniak (2000). As this experimentally determined T_C range has been corroborated by studies of natural samples investigating the T_C of Pb in rutile (Kooijman et al. 2010; Vry and Baker 2006), it is our preferred estimate, and a $T_{C\ (Pb–Rt)}$ of 550–650 °C will be used for our IVZ rutiles in the following discussion.

Comparison with previous IVZ thermochronology

The 160–180 Ma U–Pb dates obtained for IVZ rutiles in this study are in broad agreement with previously published U–Pb geochronology of rutile from the IVZ, but with some important differences. Zack et al. (2011) obtained an age of 181 ± 4 Ma for the largest (>200 μm) rutiles from one Val d'Ossola sample and stated that a grainsize dependence existed for their rutile U–Pb ages. However, they presented data only for the largest (and thus oldest) rutiles. Their 181 ± 4 Ma age is within the range of individual dates from this study, which tail up to ~180 Ma in most samples (Fig. 5a–g), although we do not observe a dependence of age on the position of spots within each grain. Given that Zack et al. (2011) considered exclusively the oldest grains, their ages would be expected to be at the older end of our spectrum of individual dates. Furthermore, their age is in agreement with our ~175 Ma age populations (Fig. 7).

The rutile U–Pb depth profiles of Smye and Stockli (2014) for two samples from Val d'Ossola show a rapid increase in U–Pb dates from ~140 Ma to ~180 Ma in the outermost 15 μm of grains and then a plateau at 180–190 Ma. This age distribution differs from that observed for our single spot rutile U–Pb dates, where we obtain 160–180 Ma dates at distances of 10–200 μm from the apparent grain edge, with no relationship between date and position. Smye and Stockli (2014) also performed single spot analyses on polished rutiles from the same samples, for comparison with their depth profiling results. Their single spot data (taken from their supplementary material DR1)

show a similar age distribution to ours, with scattered dates between ~150 and ~190 Ma, occasionally up to ~210 Ma, and no relationship between date and position within the grain (Fig. S3). Probability density functions that we constructed for their single spot dates are complex with multiple age peaks (Fig. S4), much like for our samples, and with a similar age distribution. Using Isoplot Ex 3.5, we obtained weighted mean $^{206}Pb/^{238}U$ ages of 170 ± 2 Ma and 185 ± 4 Ma for the single spot analyses of these two samples. The 170 ± 2 Ma age is comparable to ages of our samples, but significantly younger than the plateau ages of Smye and Stockli's (2014) depth profiles, reflecting a greater dominance of younger ages in their single spot analyses than seen in their depth profiles. This weighted mean age remains ~170 Ma even if only selected analyses (e.g. only core domains) are included. The significant difference between age distributions from depth profiling versus both our and Smye and Stockli's (2014) single spot U–Pb dates suggests that the two techniques are recording different information.

Compared to samples from a similar position in the crustal section, the 160–180 Ma U–Pb ages of IVZ rutiles are distinctly younger than 210–240 Ma Ar–Ar hornblende ages in Val Strona (Boriani and Villa 1997; Siegesmund et al. 2008) and are also younger than the >247 Ma Ar–Ar hornblende ages determined on late-magmatic amphiboles for the Paleozoic Anzola gabbro (Brodie et al. 1989; Fig. 7). The U–Pb rutile ages are similar to or only slightly older than 160–170 Ma K–Ar biotite ages in Val Strona and Val d'Ossola (Siegesmund et al. 2008; Wolff et al. 2012; Fig. 7).

Rutile age interpretation

The 160–180 Ma U–Pb dates of IVZ rutiles are substantially younger than both regional amphibolite–granulite facies metamorphism (316 ± 3 Ma; Ewing et al. 2013) and high-temperature contact metamorphism associated with the emplacement of the Mafic Complex (at 288 ± 4 Ma; Peressini et al. 2007). Rutile formed as part of the same reaction that produced garnet and partial melt during these Permian high-temperature metamorphic events (e.g. Luvizotto and Zack 2009; Schnetger 1994). Formation of rutile during peak temperatures in the Permian is confirmed by the 900–930 °C peak temperatures recorded by Zr thermometry for populations of IVZ rutiles from the same samples (Ewing et al. 2013). Rutile U–Pb dates clearly do not record formation, but rather cooling through the closure temperature of Pb in rutile. This is expected, given that $T_{C\ (Pb–Rt)}$ is low (550–650 °C) compared to the peak metamorphic temperatures of >900 °C experienced by these samples during Permian metamorphism. All IVZ samples also have a significant population of Zr-in-rutile temperatures at 750–800 °C (Ewing et al. 2013). The observation of numerous small (5–10 μm) zircons surrounding rutile with 750–800 °C temperatures led Ewing et al. (2013) to suggest that these grains were recrystallised at these temperatures, with expulsion of the excess Zr produced to form the small zircons, arguing against growth of a distinct population of rutiles during later retrograde evolution. As the last recrystallisation of rutile occurred at temperatures well above $T_{C\ (Pb–Rt)}$, U–Pb ages will record subsequent cooling through this temperature even in recrystallised rutiles.

Although our rutile analyses sampled a continuous range of effective radii from 10–200 μm (Fig. 6a), most samples have probability density functions that partially resolve two discrete age populations. This suggests that the observed range of rutile U–Pb dates is not simply the result of grainsize-controlled differences in closure temperature and that the two age populations extracted from the data record real, distinct events. The fact that there is no relationship between U–Pb dates and distance from the edge of the rutile, nor a resolvable difference in age between core and rim of individual rutiles, also strongly argues against grainsize-controlled differences in closure temperature as the explanation of the observed range of rutile U–Pb dates, suggesting that smaller diffusion lengths may have controlled Pb loss (see discussion below). Importantly, the preservation of peak (i.e. Paleozoic) Zr-in-rutile temperatures by many of the dated rutiles, including some that gave the youngest U–Pb ages, unequivocally rules out complete recrystallisation (e.g. dissolution–reprecipitation) of some rutiles to explain the range of U–Pb ages measured. That the age populations extracted by the unmix ages algorithm are meaningful is supported by the excellent agreement of unmixed ages between samples for both the older and younger populations. This echoes the similarity in age distributions already qualitatively observed in probability density functions, demonstrating that the unmix ages algorithm has reliably quantified these age peaks (Fig. 5a–g).

The younger of the rutile U–Pb age populations dates the cooling of the IVZ crustal section, for the last time, below 550–650 °C at 160 ± 7 Ma. The older 176 ± 8 Ma age population is interpreted to record earlier cooling through the same temperature range. The presence of both age populations could be explained by rapid reheating followed by renewed cooling occurring at 160 ± 7 Ma, with the ~160 Ma heating event affecting the U–Pb ages of only some rutiles. The resetting of U–Pb dates in some rutiles and not others within each sample could be controlled, for example, by some (but not all) rutile grains having diffusion domain lengths dramatically smaller than the grainsize due to exsolution lamellae or subgrain boundaries that are not easily detectable. Diffusive loss of Pb from rutiles with such reduced diffusion domains would occur at a lower temperature than from rutiles where the grainsize

represents the diffusion domain, thus allowing resetting of one but not the other during reheating to a temperature intermediate between the closure temperatures of the two domain scales. Such a difference in exsolution or subgrain domain formation could, for example, stem from different processes affecting rutile in restitic and leucosome layers, although this is speculative. Preservation of both age populations would be facilitated by rapid rates of heating and cooling, as this would impede the complete re-equilibration of the U–Pb system in rutile in the second heating event. This possibility and its implications will be examined in the context of the tectonothermal evolution of the IVZ in the following section.

One of the striking features of the U–Pb data presented here is the consistency of rutile ages, both at ~160 and ~175 Ma, throughout the IVZ (Figs. 5, 7). The dated samples cover an area from Val Sessera in the south to Val d'Ossola in the north, which represents ~35 km along the strike of the IVZ (Fig. 1). They cover a relatively narrow range in former depth in the crust, as the occurrence of rutile is restricted to the highest-grade metapelites in the IVZ. However, the samples do include both granulite facies Kinzigite Formation metapelites, and a septum in the Mafic Complex. The consistency of rutile U–Pb ages of seven samples along the length of the IVZ demonstrates that the cooling they record occurred synchronously on a regional scale. In the following section, we will argue that between these two episodes of regional cooling, episodic heating of the IVZ in the Jurassic occurred during continental breakup associated with the opening of the Alpine Tethys.

Constraints on the Permian to Jurassic thermal evolution of the IVZ lower crust

Several previous studies of the tectono-thermal evolution of the Ivrea Zone (e.g. Handy et al. 1999; Siegesmund et al. 2008) have assumed continuous conductive cooling following peak temperatures associated with the ~290 Ma intrusion of the Mafic Complex. However, over the past two decades, increasing evidence has mounted against this view, favouring an episodic thermal evolution with background conductive cooling punctuated (at least locally) by pulses of magmatism, fluid influx, and heating throughout the Triassic and Jurassic (e.g. Grieco et al. 2001; Lu et al. 1997; Mayer et al. 2000; Mazzucchelli et al. 2010; Morishita et al. 2008; Schaltegger et al. 2015; Stähle et al. 1990; Zanetti et al. 2013, and see Sect. 2).

To construct a more complete picture of the thermal evolution of the IVZ in the lead up to the Jurassic stages recorded by our new rutile U–Pb ages, we briefly review existing data from the literature that can be used to constrain reheating events within the IVZ. Regional correlations between IVZ data and the tectonic evolution of the rest of the Southern Alps provide important insights into the link between surface and deep-seated processes along the northern end of the Adriatic plate from the Paleozoic onwards, although further work is required to fully characterise the extent of each thermal pulse outlined in Fig. 8 and to test whether the episodic nature of this tectono-thermal evolution is over-emphasised by sampling bias.

A first reheating can be proposed at ~260 Ma (Fig. 8), based on the widespread occurrence of recrystallised zircon domains with this age in both amphibolite and granulite facies metapelites from the IVZ (Ewing et al. 2013; Vavra et al. 1999). ~260 Ma is the dominant age peak for all three zircon samples U–Pb dated by Ewing et al. (2013), and zircons from a Val Mastallone septum yielded Ti-in-zircon temperatures of 770 ± 30 °C at 259 ± 3 Ma (Ewing et al. 2013). This temperature–time constraint cannot be reconciled with simple conductive cooling from the time of the Mafic Complex intrusion, as fitting a typical error-function-type cooling curve through it would imply steady-state temperatures of ~750 °C, considerably hotter than the ~600 °C temperatures expected for the base of thermally undisturbed, stable Adriatic continental crust (Müntener et al. 2000). Furthermore, the fact that ~260 Ma ages are observed even in zircons from amphibolite facies metapelites (Vavra et al. 1999) implies that this zircon recrystallisation event was widespread throughout the crustal section and not restricted to the proximity of the Mafic Complex. Therefore, Ewing et al. (2013) proposed that the recrystallisation of zircons at ~260 Ma could be explained by delayed conductive heating related to the raised asthenosphere associated with the previous emplacement of the Mafic Complex. In an analogous fashion, in the Val Malenco crust–mantle transition (Central Alps, Italy), metamorphism at ~260 Ma followed intrusion of gabbros at ~280 Ma and has been attributed to conductive heating due to the slow migration of a thermal anomaly produced by the shallow asthenosphere associated with mantle-derived magmatism (Hermann and Rubatto 2003). This suggests that heating at ~260 Ma in the IVZ may be part of a wider regional-scale tectono-thermal event, consistent with the well-documented waning stages of regional transtensional deformation at 270–260 Ma recorded throughout the Southern Alps (northern Italy) prior to the onset of the Tethyan sedimentary cycle (Cassinis et al. 2012).

A significant post-Permian episode of heating and fluid influx is inferred in the Middle Triassic, based on existing U–Pb zircon data from throughout the IVZ. Intrusion of the Finero Mafic Complex in the northern IVZ has recently been constrained to 232 ± 3 Ma (Zanetti et al. 2013), recording voluminous magmatism in the Ladinian. Sporadic Middle Triassic (~240 Ma) ages for recrystallised domains of zircons from IVZ metapelites, even at considerable distances from Finero, attest to associated episodic

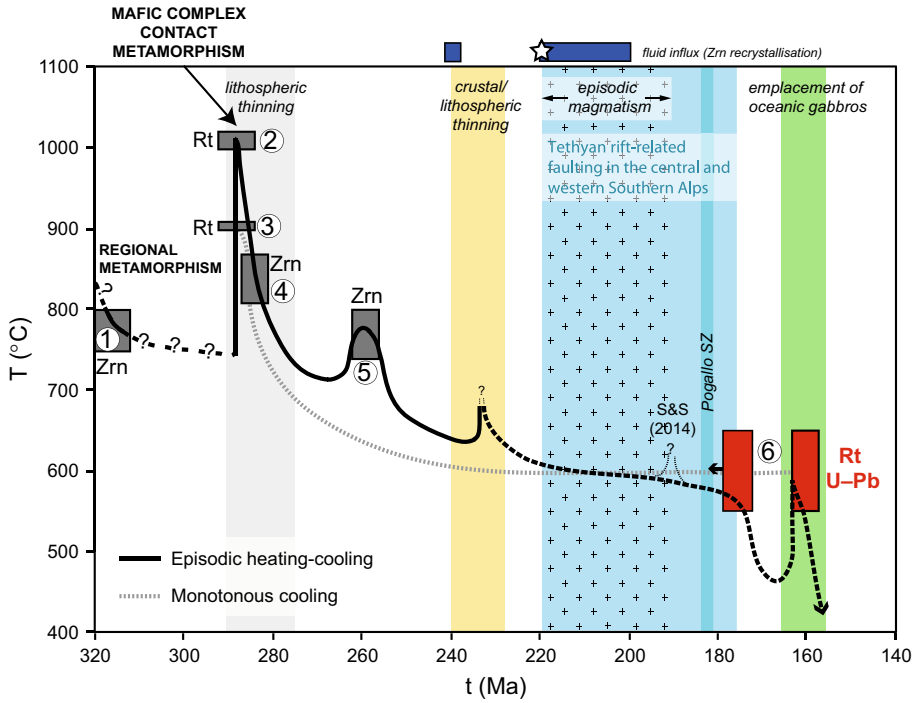

Fig. 8 Proposed temperature–time (T–t) path for the westernmost part of the IVZ section. T–t constraints (*1–5*) and T–t path until Mafic Complex emplacement are from Ewing et al. (2013). Constraints from U–Pb geochronology of rutile (this study) are shown as red boxes distinguishing the older and younger age populations, for a T_C of Pb in rutile (*6*) determined from experimental diffusion data (Cherniak 2000). Episodic cooling and reheating (*black line*) is the preferred interpretation (see text for discussion of the timing of proposed heating pulses). *Dashed lines* indicate less precisely constrained parts of the T–t evolution. The t spike marked "S&S (2014)" indicates the early Jurassic thermal pulse inferred by Smye and Stockli (2014) based on in-diffusion of Zr into rutiles, plotted at very approximate T and t, as neither was precisely constrained in that study. Our data cannot confirm or constrain this heating event. A simple monotonous cooling path (*grey dashed line*) is shown for comparison. *Yellow band* marks a period of widespread crustal extension/lithospheric thinning in the Southern Alps in the Triassic (Gaetani 2010). *Band of crosses* marks a period of episodic mantle-derived magmatism and metasomatism (Grieco et al. 2001; Lu et al. 1997; Mayer et al. 2000; Mazzucchelli et al. 2010; Morishita et al. 2008; Schaltegger et al. 2015; Stähle et al. 1990; Zanetti et al. 2013). *Pale blue band* marks the period of Tethyan rift-related faulting in the Southern Alps (Berra et al. 2009; Bertotti et al. 1993); *medium blue band* marks the timing of movement on the Pogallo shear zone (SZ) (Mulch et al. 2002a). *Green band* delineates the timing of emplacement of the majority of Tethyan oceanic gabbros (Bill et al. 1997; Kaczmarek et al. 2008; Li et al. 2013; Liati et al. 2005; Rubatto et al. 1998; Rubatto and Scambelluri 2003; Schaltegger et al. 2002). *Dark blue bars* delineate periods of fluid influx inferred from zircon recrystallisation ages of Ewing et al. (2013), with a star indicating the most dominant age

fluid influx at this time throughout the IVZ (Ewing et al. 2013; Peressini et al. 2007; Vavra et al. 1999). This stage of fluid influx and deep-seated magmatism is contemporaneous with the emplacement of magma bodies and lava flows throughout the Dolomites, in the Southern Alps (see Gaetani 2010). The high subsidence rates recorded in the eastern part of the Southern Alps in the Ladinian, combined with evidence for magmatism, are compatible with marked lithospheric thinning, although the exact geodynamic setting is debated (see Gaetani 2010 and Zanetti et al. 2013).

A further episode of magmatism and fluid activity in the Late Triassic—Early Jurassic is recorded by widespread fluid-mediated recrystallisation of pre-existing zircon domains at 220–200 Ma in some IVZ metapelites (Ewing et al. 2013; Vavra et al. 1999), with a dominance of ~220 Ma ages (see Fig. 7 of Ewing et al. 2013). The sporadic influx of fluids at 220–200 Ma is consistent with the occurrence of episodic mantle-derived magmatism and associated metasomatism in the northern IVZ from ~220 to 190 Ma (Grieco et al. 2001; Morishita et al. 2008; Schaltegger et al. 2015; Stähle et al. 1990), as described in detail in Sect. 2. This time period coincides with the onset of extensional faulting related to the opening of the Alpine Tethys as recorded in the Southern Alpine cover sequence by the development of the Lombardian Basin at 220–180 Ma (Bertotti et al. 1993). Crustal thinning towards the end of this interval is also documented by the activity of extensional shear zones within the IVZ itself (e.g. Mulch et al. 2002a).

Following the onset of regional extensional faulting in the Lombardian basin, crustal thinning within the Southern Alps was progressively localised in westerly domains (Bertotti et al. 1993; Berra et al. 2009), eventually culminating in complete crustal excision and regional exhumation

of subcontinental mantle to the seafloor, constrained to 167–155 Ma throughout the Alpine Tethys (e.g. Bill et al. 2001; Chiari et al. 2000). Jurassic lithospheric thinning was accompanied by emplacement and solidification of magma within the sub-continental mantle. Most intrusive magmatism throughout the different parts of the Alpine Tethys now sampled in Mediterranean orogenic belts is constrained to 166–158 Ma (Bill et al. 1997; Kaczmarek et al. 2008; Li et al. 2013; Liati et al. 2005; Rubatto et al. 1998; Rubatto and Scambelluri 2003; Schaltegger et al. 2002), although older ages starting from ~180 Ma have been determined locally (Rampone et al. 2014; Tribuzio et al. 2004).

Within this context, the dominant ~160 Ma population of rutile U–Pb ages postdates the 220–180 Ma main rifting phase and coincides with the formation of the first Tethyan oceanic crust and associated gabbros at 166–158 Ma, following the termination of rifting (Figs. 7, 8). This population of rutile ages, recorded by lower-retentivity rutile domains, records cooling following rapid reheating at ~160 Ma, subsequent to an earlier cooling stage that is recorded by higher-retentivity rutile grains. Several lines of evidence indicate that the Jurassic cooling of the IVZ recorded by our ~160 Ma rutile U–Pb ages followed regional episodic reheating of the crustal section, rather than simple slow monotonous cooling. Firstly, the samples studied here span a considerable proportion of the length of the IVZ (>35 km along the strike of the Paleozoic HT foliation) and, most importantly, come from different original depths within the Paleozoic crust. Although the width of the sampling area is limited by the original occurrence and preservation of rutile, the studied samples span a distance between 1.5 and 5.0 km from the Insubric line, indicating that cooling occurred contemporaneously (within error) across different former crustal depths. Secondly, within the IVZ, the latest activity of ductile shear zones is constrained to the Lower Jurassic, at ~182 Ma (Mulch et al. 2002a), while normal faulting in the neighbouring westernmost Serie dei Laghi is constrained to the Pliensbachian–Toarcian (Berra et al. 2009). All documented rift-related fault activity thus pre-dates our U–Pb rutile ages by ~15 Ma, suggesting that cooling through 550–650 °C at ~160 Ma cannot be associated with rift-related exhumation. This is further supported by the absence of any documented rift-related shear zone in Val Sessera, where two of our samples originated. In the context of the beginning of sea-floor spreading and the termination of rifting, the Middle Jurassic regional cooling recorded by the main population of ~160 Ma rutile U–Pb ages is best explained by an early post-rift (syn-drift) episode of heating and cooling of the distal part of the Adriatic margin (Fig. 2), with only a minor role played by exhumation-related conductive cooling. A similar heating–cooling cycle broadly coeval with the rift-to-drift transition has recently been proposed for the hyper-extended Cretaceous margins now sampled in the Pyrenees (Vacherat et al. 2014). The contemporaneity with the well-documented onset of mantle exhumation and extensive MORB magmatism in the Alpine Tethys (e.g. Bill et al. 1997; Kaczmarek et al. 2008; Li et al. 2013; Liati et al. 2005; Rubatto et al. 1998; Rubatto and Scambelluri 2003; Schaltegger et al. 2002) suggests that early post-rift heating and cooling of the IVZ, which was located at the transition between the proximal and distal Adriatic margin (Fig. 2), was probably related to lithospheric thinning and the associated occurrence of a shallow asthenosphere. Our data are in good agreement with recent results from thermo-mechanical modelling on the formation of passive margins (Brune et al. 2014). These models show that lower crust will first undergo cooling due to exhumation, followed by a period of heating during the formation of hyper-extended crust when asthenospheric mantle is emplaced at shallow levels. The modelled timeframe for this evolution is of 10–20 My (Brune et al. 2014), consistent with our age data. With the subsequent onset of formation of oceanic crust, lithospheric-scale thermal relaxation along the distal Adriatic margin, probably due to increasing distance from these heat sources, allowed final cooling below the closure temperature of Pb in rutile. This cooling is likely to have been relatively rapid, so the postulated heating event can be inferred to have occurred just before ~160 Ma. Rapid cooling following the heating pulse would be consistent with the fact that K–Ar biotite ages are similar to U–Pb rutile ages from the same area in the IVZ (Siegesmund et al. 2008 and this study; Fig. 2) in spite of this system's much lower closure temperature. However, because excess Ar cannot be detected in K–Ar ages, these should be interpreted with caution.

The older ~175 Ma population of rutile U–Pb ages is interpreted to record an earlier episode of cooling through the T_C of 550–650 °C that has only been partially erased by subsequent heating at ~160 Ma. A distinct cooling event is indicated by the discrete age populations identified in most samples with no relationship between age and grainsize, in spite of the fact that a large and continuous range of grainsizes were analysed. It cannot be excluded that a grainsize–age relationship not resolved at the precision of our in situ analyses is also superimposed on these discrete cooling events, adding further complexity to the data. We postulate that the ~175 Ma cooling may be due to rift-related exhumation, which would be consistent with the fact that the ~175 Ma ages coincide with or only slightly postdate the termination of documented rift-related activity of faults and shear zones in the western Southern Alps (Berra et al. 2009; Mulch et al. 2002a).

Our data do not allow us to precisely constrain the onset of cooling due to rift-related exhumation, which may have begun some time prior to the closure of the U–Pb system in

rutile depending on the background temperature and cooling rate. The rutile U–Pb data are also unable to resolve whether earlier heating–cooling cycles affected the IVZ crustal section prior to this final one. However, U–Pb geochronology of rutile demonstrates unequivocally that episodic crustal reheating terminated at ~160 Ma, and the IVZ lower crust did not experience temperatures above 550–650 °C after this time (Fig. 8).

Our finding of rapid cooling at or just before ~175 Ma is in good agreement with the results of Smye and Stockli (2014), who inferred rapid cooling at ~180 Ma from their U–Pb depth profiling of rutile. The reheating at ~160 Ma indicated by our rutile U–Pb data is however in conflict with the thermal evolution proposed by Smye and Stockli (2014) based on numerical inversion of their age profiles, which did not detect any heating event at this time. This difference in inferred thermal history stems from the different age distributions recorded by depth profiling and spot analyses, as discussed in the preceding section. The dominance of 160–170 Ma dates over ~180 Ma dates in Smye and Stockli's (2014) spot analyses of one sample (Fig S3) suggests that rutile from this sample also records an event younger than ~180 Ma, even if it was not detected by the depth profiling, supporting our inference of a heating event at this time.

Implications for rutile geochemistry

This study demonstrates that valuable thermochronological constraints can be obtained from U–Pb dating of rutile. The rutile U–Pb dataset presented here gives internally consistent ages covering most of the length of the IVZ, providing an unambiguous temporal constraint on the Jurassic rift-related thermal evolution of this widely studied lower crustal section. In a high-temperature setting such as the IVZ, the fact that Zr-in-rutile thermometry can be used to rule out recrystallisation of rutile as a cause of reset U–Pb ages is a valuable tool to test and strengthen thermochronologic interpretations.

The simple, internally consistent dataset provided by U–Pb geochronology of rutile in the IVZ is in contrast to the complex and sometimes contradictory datasets provided by other thermochronometers such as ^{40}Ar–^{39}Ar in hornblende (Fig. 7). This at least partly reflects the importance of recrystallisation in the resetting of ^{40}Ar–^{39}Ar ages, instead of (or as well as) diffusive loss of Ar (e.g. Villa 1998). The two geochronometers thus have the potential to date different processes and so provide complementary information, with U–Pb ages of rutile controlled (at least in this case) strictly by diffusive loss of Pb during cooling, while deformation-driven recrystallisation of hornblende may play an important role in resetting of ^{40}Ar–^{39}Ar.

In the IVZ, Zr-in-rutile temperatures record the thermal maximum at ultra-high temperatures of >900 °C (Ewing et al. 2013), whereas rutile U–Pb ages record cooling through 550–650 °C some 120 Ma later. The decoupling of these systems at high temperatures, which is predicted by experimental diffusion data for Pb and Zr in rutile (Cherniak et al. 2007; Cherniak and Watson 2000), demands caution in applying coupled Zr thermometry and U–Pb geochronology to out-of-context rutiles such as detrital grains (e.g. Meinhold et al. 2011). In the simplest case of monotonous cooling, rutile U–Pb ages will postdate Zr temperatures by a period dictated only by the cooling rate and initial temperature. However, our IVZ case study demonstrates that much greater complexity can be encountered in the case of episodic cooling and reheating, leading to significant time lags between Zr temperatures and U–Pb ages of rutile and requiring independent data to deconvolve the intervening history. In well-constrained settings such as the IVZ, this decoupling can be exploited to obtain information about two distinct parts of the metamorphic evolution from the same mineral.

Conclusions

Seven granulite facies metapelites from throughout the former base of the Ivrea–Verbano Zone lower crust record two populations of rutile U–Pb ages at 176 ± 8 Ma and 160 ± 7 Ma. U–Pb ages from each population are indistinguishable between samples, which span much of the length of the IVZ. Both age populations record synchronous cooling through the 550–650 °C closure temperature of Pb in rutile on a regional scale, presenting a more coherent dataset than other thermochronometers in the IVZ. The ~160 Ma age population is dominant and records the final cooling of the crustal section below 550–650 °C. This group of ages postdates rift-related extensional deformation within the Adriatic margin that preceded the opening of the Alpine Tethys ocean, but coincides with voluminous gabbroic magmatism associated with the onset of seafloor spreading. These ages cannot therefore be related to exhumation-related cooling and are instead interpreted to record an early post-rift heating–cooling cycle during oceanisation. The ~175 Ma age population coincides with the latest documented stages of activity of rift-related faults (Berra et al. 2009) and shear zones (Mulch et al. 2002a) within the western termination of the Adriatic margin. As a result, this age population is interpreted to record cooling associated with rift-related exhumation. The preservation of this older age population suggests that both the ~160 Ma heating event and subsequent cooling were rapid, facilitating incomplete re-equilibration of the U–Pb system in rutile. Our IVZ case study demonstrates the applicability of U–Pb geochronology of rutile to constraining the thermal evolution of the lower crust during post-granulitic metamorphic evolution.

Acknowledgments We thank P. Holden, T. Ireland and I. Williams for constructive discussions on geochronology by SHRIMP and analytical assistance, and introducing us to the 3-U plot (I. Williams). We thank the ANU Centre for Advanced Microscopy for access to their SEM and technical support. T. Duretz is thanked for discussions on thermal modelling. We are indebted to A. Bevan at the Western Australian Museum for providing the Wodgina rutile for characterisation as a standard. This work was financially supported by Australian Research Council grant DP0556700 and the Research School of Earth Sciences. T. Ewing was supported by APA, ANU and Jaeger scholarships at RSES, and was supported by the University of Lausanne during the preparation of this manuscript. M. Beltrando gratefully acknowledges support by the Margin Modelling Phase 3 partners (BP, Conoco Phillips, Statoil, Petrobras, Total, Shell, Hess, BHP-Billiton and BG). We thank Alberto Zanetti and an anonymous reviewer for their constructive comments that improved the manuscript, and Jochen Hoefs for editorial handling.

References

Baldwin JA, Brown M (2008) Age and duration of ultrahigh-temperature metamorphism in the Anápolis-Itauçu Complex, Southern Brasília Belt, central Brazil—constraints from U–Pb geochronology, mineral rare earth element chemistry and trace-element thermometry. J Metamorph Geol 26:213–233

Barboza SA, Bergantz GW (2000) Metamorphism and anatexis in the Mafic Complex contact aureole, Ivrea zone, northern Italy. J Petrol 41:1307–1327

Barboza SA, Bergantz GW, Brown M (1999) Regional granulite facies metamorphism in the Ivrea zone: is the Mafic Complex the smoking gun or a red herring? Geology 27:447–450

Beltrando M, Manatschal G, Mohn G, Dal Piaz GV, Vitale Brovarone A, Masini E (2014) Recognizing remnants of magma-poor rifted margins in high-pressure orogenic belts: the Alpine case study. Earth Sci Rev 131:88–115

Berra F, Galli MT, Reghellin F, Torricelli S, Fantoni R (2009) Stratigraphic evolution of the Triassic-Jurassic succession in the Western Southern Alps (Italy): the record of the two-stage rifting on the distal passive margin of Adria. Basin Res 21:335–353

Bertotti G, Picotti V, Bernoulli D, Castellarin A (1993) From rifting to drifting: tectonic evolution of the South-Alpine upper crust from the Triassic to the Early Cretaceous. Sed Geol 86:53–76

Bill M, Bussy F, Cosca M, Masson H, Hunziker JC (1997) High-precision U-Pb and $^{40}Ar/^{39}Ar$ dating of an Alpine ophiolite (Gets nappe, French Alps). Eclogae Geol Helv 90:43–54

Bill M, O'Dogherty L, Guex J, Baumgartner PO, Masson H (2001) Radiolarite ages in Alpine-Mediterranean ophiolites: constraints on the oceanic spreading and the Tethys-Atlantic connection. Geol Soc Am Bull 113:129–143

Blackburn T, Bowring SA, Schoene B, Mahan K, Dudas F (2011) U-Pb thermochronology: creating a temporal record of lithosphere thermal evolution. Contrib Miner Petrol 162:479–500

Boriani A, Burlini L (1995) Carta geologica della Valle Cannobina. Dipartimento di scienze della terra dell'Università degli studi di Milano

Boriani A, Giobbi E (2004) Does the basement of western southern Alps display a tilted section through the continental crust? A review and discussion. Periodico di Mineralogia 73:5–22

Boriani AC, Villa IM (1997) Geochronology of regional metamorphism in the Ivrea-Verbano Zone and Serie dei Laghi, Italian Alps. Schweiz Miner Petrogr Mitt 77:381–401

Boriani A, Burlini L, Sacchi R (1990) The Cossato-Mergozzo-Brissago Line and the Pogallo Line (Southern Alps, Northern Italy) and their relationships with the late-Hercynian magmatic and metamorphic events. Tectonophysics 182:91–102

Boston K, Rubatto D, Hermann J, Amelin Y, Engi M (2013) Relating U–Th–Pb ages of accessory minerals to metamorphism: a case study from the Barrovian sequence of the Central Alps, Switzerland. Mineral Mag 77:747

Brenan JM, Shaw HF, Phinney DL, Ryerson FJ (1994) Rutile-aqueous fluid partitioning of Nb, Ta, Hf, Zr, U and Th: implications for high-field strength element depletions in island-arc basalts. Earth Planet Sci Lett 128:327–339

Brodie KH, Rutter EH (1987) Deep crustal extensional faulting in the Ivrea Zone of northern Italy. Tectonophysics 140:193–212

Brodie KH, Rex D, Rutter EH (1989) On the age of deep crustal extensional faulting in the Ivrea zone, northern Italy, Alpine tectonics. Geol Soc Spec Publ 45:203–210

Brune S, Heine C, Pérez-Guissinyé M, Sobolev SV (2014) Rift migration helps explain continental margin asymmetry and crustal hyper-extension. Nat Commun 5, doi:10.1038/ncomms5014

Cassinis G, Perotti C, Ronchi A (2012) Permian continental basins in the Southern Alps (Italy) and peri-mediterranean correlations. Int J Earth Sci 101:129–157

Cherniak DJ (1993) Lead diffusion in titanite and preliminary results on the effects of radiation damage on Pb transport. Chem Geol 110:177–194

Cherniak DJ (2000) Pb diffusion in rutile. Contrib Miner Petrol 139:198–207

Cherniak DJ, Watson EB (2000) Pb diffusion in zircon. Chem Geol 172:5–24

Cherniak DJ, Manchester J, Watson EB (2007) Zr and Hf diffusion in rutile. Earth Planet Sci Lett 261:267–279

Chiari M, Marcucci M, Principi G (2000) The age of the radiolarian cherts associated with the ophiolites in the Apennines (Italy) and Corsica (France): a revision. Ofioliti 25:141–146

Clark DJ, Hensen BJ, Kinny PD (2000) Geochronological constraints for a two-stage history of the Albany-Fraser Orogen, Western Australia. Precambr Res 102:155–183

Corfu F, Easton RM (2001) U-Pb evidence for polymetamorphic history of Huronian rocks within the Grenville front tectonic zone east of Sudbury, Ontario, Canada. Chem Geol 172:149–171

Demarchi G, Quick J, Sinigoi S, Mayer A (1998) Pressure gradient and original orientation of a lower-crustal intrusion in the Ivrea-Verbano Zone, northern Italy. J Geol 106:609–621

Ernst WG, Liu J (1998) Experimental phase-equilibrium study of Al- and Ti-contents of calcic amphibole in MORB—a semiquantitative thermobarometer. Am Mineral 83:952–969

Ewing TA (2011) Hf isotope analysis and U–Pb geochronology of rutile: technique development and application to a lower crustal section (Ivrea-Verbano Zone, Italy). Unpublished Ph.D. thesis, Australian National University, p 385

Ewing TA, Rubatto D, Hermann J (2013) The robustness of the Zr-in-rutile and Ti-in-zircon thermometers during high-temperature metamorphism (Ivrea-Verbano Zone, northern Italy). Contrib Miner Petrol 165:757–779

Ewing TA, Rubatto D, Hermann J (2014) Hafnium isotopes and Zr/Hf of rutile and zircon from lower crustal metapelites (Ivrea-Verbano Zone, Italy): implications for chemical differentiation of the crust. Earth Planet Sci Lett 389:106–118

Flowers RM, Mahan KH, Bowring SA, Williams ML, Pringle MS, Hodges KV (2006) Multistage exhumation and juxtaposition of lower continental crust in the western Canadian Shield: Linking high-resolution U–Pb and $_{40}Ar/_{39}Ar$ thermochronometry with pressure-temperature-deformation paths. Tectonics 25:TC4003. doi:10.1029/2005TC001912

Foley SF, Barth MG, Jenner GA (2000) Rutile/melt partition coefficients for trace elements and an assessment of the influence

of rutile on the trace element characteristics of subduction zone magmas. Geochim Cosmochim Acta 64:933–938

Frost BR, Chamberlain KR, Schumacher JC (2001) Sphene (titanite): phase relations and role as a geochronometer. Chem Geol 172:131–148

Gaetani M (2010) From Permian to Cretaceous: Adria as pivotal between extensions and rotations of Tethys and Atlantic Oceans In: Beltrando M, Peccerillo A, Mattei M, Conticelli S, Doglioni C (eds) J Virtual Explor 36 (6) doi:10.3809/jvirtex.2010.00235

Grieco G, Ferrario A, Von Quadt A, Koeppel V, Mathez EA (2001) The zircon-bearing chromitites of the phlogopite peridotite of Finero (Ivrea zone, Southern Alps): evidence and geochronology of a metasomatized mantle slab. J Petrol 42:89–101

Handy MR (1987) The structure, age and kinematics of the Pogallo fault zone - Southern Alps, northwestern Italy. Eclogae Geol Helv 80:593–632

Handy MR, Franz L, Heller F, Janott B, Zurbriggen R (1999) Multistage accretion and exhumation of the continental crust (Ivrea crustal section, Italy and Switzerland). Tectonics 18:1154–1177

Henk A, Franz L, Teufel S, Oncken O (1997) Magmatic underplating, extension, and crustal reequilibration: insights from a cross-section through the Ivrea Zone and Strona-Ceneri Zone, northern Italy. J Geol 105:367–377

Hermann J, Rubatto D (2003) Relating zircon and monazite domains to garnet growth zones: age and duration of granulite facies metamorphism in the Val Malenco lower crust. J Metamorph Geol 21:833–852

Kaczmarek MA, Müntener O, Rubatto D (2008) Trace element chemistry and U-Pb dating of zircons from oceanic gabbros and their relationship with whole rock composition (Lanzo, Italian Alps). Contrib Miner Petrol 155:295–312

Klötzli US, Sinigoi S, Quick JE, Demarchi G, Tassinari CCG, Sato K, Günes Z (2014) Duration of igneous activity in the Sesia Magmatic System and implications for high-temperature metamorphism in the Ivrea-Verbano deep crust. Lithos 206–207:19–33

Kooijman E, Mezger K, Berndt J (2010) Constraints on the U–Pb systematics of metamorphic rutile from in situ LA-ICP-MS analysis. Earth Planet Sci Lett 293:321–330

Kooijman E, Smit MA, Mezger K, Berndt J (2012) Trace element systematics in granulite facies rutile: implications for Zr geothermometry and provenance studies. J Metamorph Geol 30:397–412

Li QL, Li SG, Zheng YF, Li HM, Massonne HJ, Wang QC (2003) A high precision U-Pb age of metamorphic rutile in coesite-bearing eclogite from the Dabie Mountains in central China: a new constraint on the cooling history. Chem Geol 200:255–265

Li X-H, Faure M, Lin W, Manatschal G (2013) New isotopic constraints on age and magma genesis of an embryonic oceanic crust: the Chenaillet Ophiolite in the Western Alps. Lithos 160–161:283–291

Liati A, Froitzheim N, Fanning CM (2005) Jurassic ophiolites within the Valais domain of the Western and Central Alps: geochronological evidence for re-rifting of oceanic crust. Contrib Miner Petrol 149:446–461

Liu J, Bohlen SR, Ernst WG (1996) Stability of hydrous phases in subducting oceanic crust. Earth Planet Sci Lett 143:161–171

Lu MH, Hofmann AW, Mazzucchelli M, Rivalenti G (1997) The mafic-ultramafic complex near Finero (Ivrea-Verbano Zone), II. Geochronology and isotope geochemistry. Chem Geol 140:223–235

Ludwig KR (2001) Squid 1.02 - A user′s manual, Berkeley Geochronology Center Special Publication No. 2

Ludwig KR (2003) User's manual for Isoplot 3.00: a geochronological toolkit for Microsoft Excel, Berkeley Geochronology Center Special Publication No. 4

Luvizotto GL, Zack T (2009) Nb and Zr behavior in rutile during high-grade metamorphism and retrogression: an example from the Ivrea-Verbano Zone. Chem Geol 261:303–317

Mayer A, Mezger K, Sinigoi S (2000) New Sm-Nd ages for the Ivrea-Verbano Zone, Sesia and Sessera valleys (Northern-Italy). J Geodyn 30:147–166

Mazzucchelli M, Zanetti A, Rivalenti G, Vannucci R, Correia CT, Gaeta Tassinari CC (2010) Age and geochemistry of mantle peridotites and diorite dykes from the Baldissero body: insights into the Paleozoic-Mesozoic evolution of the Southern Alps. Lithos 119:485–500

Meinhold G, Morton AC, Fanning CM, Whitham AG (2011) U-Pb SHRIMP ages of detrital granulite-facies rutiles: further constraints on provenance of Jurassic sandstones on the Norwegian margin. Geol Mag 148:473–480

Mezger K, Hanson GN, Bohlen SR (1989) High-precision U-Pb ages of metamorphic rutile—application to the cooling history of high-grade terranes. Earth Planet Sci Lett 96:106–118

Mohn G, Manatschal G, Müntener O, Beltrando M, Masini E (2010) Unravelling the interaction between tectonic and sedimentary processes during lithospheric thinning in the Alpine Tethys margins. Int J Earth Sci 99:75–101

Mohn G, Manatschal G, Beltrando M, Masini E, Kusznir N (2012) Necking of continental crust in magma-poor rifted margins: evidence from the fossil Alpine Tethys margins. Tectonics 31:TC1012. doi:10.1029/2011TC002961

Morishita T, Hattori KH, Terada K, Matsumoto T, Yamamoto K, Takebe M, Ishida Y, Tamura A, Arai S (2008) Geochemistry of apatite-rich layers in the Finero phlogopite-peridotite massif (Italian Western Alps) and ion microprobe dating of apatite. Chem Geol 251:99–111

Mulch A, Cosca MA, Handy MR (2002a) In-situ UV-laser $^{40}Ar/^{39}Ar$ geochronology of a micaceous mylonite: an example of defect-enhanced argon loss. Contrib Miner Petrol 142:738–752

Mulch A, Rosenau M, Dorr W, Handy MR (2002b) The age and structure of dikes along the tectonic contact of the Ivrea-Verbano and Strona-Ceneri Zones (southern Alps, Northern Italy, Switzerland). Schweiz Mineral Petrogr Mitt 82:55–76

Müntener O, Hermann J, Trommsdorff V (2000) Cooling history and exhumation of lower-crustal granulite and upper mantle (Malenco, Eastern Central Alps). J Petrol 41:175–200

Peressini G, Quick JE, Sinigoi S, Hofmann AW, Fanning M (2007) Duration of a large Mafic intrusion and heat transfer in the lower crust: a SHRIMP U-Pb zircon study in the Ivrea-Verbano Zone (Western Alps, Italy). J Petrol 48:1185–1218

Quick JE, Sinigoi S, Mayer A (1994) Emplacement dynamics of a large mafic intrusion in the lower crust, Ivrea-Verbano Zone, northern Italy. J Geophys Res Solid Earth 99:21559–21573

Quick JE, Sinigoi S, Snoke AW, Kalakay TJ, Mayer A, Peressini G (2003) Geologic Map of the Southern Ivrea-Verbano Zone, Northwestern Italy, Geologic Investigations Series Map I-2776 and booklet [22p]. Government Printing Office, US Geological Survey, U.S

Quick JE, Sinigoi S, Peressini G, Demarchi G, Wooden JL, Sbisà A (2009) Magmatic plumbing of a large Permian caldera exposed to a depth of 25 km. Geology 37:603–606

Rampone E, Borghini G, Romairone A, Abouchami W, Class C, Goldstein SL (2014) Sm–Nd geochronology of the Erro-Tobbio gabbros (Ligurian Alps, Italy): insights into the evolution of the Alpine Tethys. Lithos 205:236–246

Redler C, Johnson TE, White RW, Kunz BE (2012) Phase equilibrium constraints on a deep crustal metamorphic field gradient: metapelitic rocks from the Ivrea Zone (NW Italy). J Metamorph Geol 30:235–254

Redler C, White RW, Johnson TE (2013) Migmatites in the Ivrea Zone (NW Italy): constraints on partial melting and melt loss in metasedimentary rocks from Val Strona di Omegna. Lithos 175:40–53

Rubatto D, Hermann J (2001) Exhumation as fast as subduction? Geology 29:3–6

Rubatto D, Scambelluri M (2003) U-Pb dating of magmatic zircon and metamorphic baddeleyite in the Ligurian eclogites (Voltri Massif, Western Alps). Contrib Miner Petrol 146:341–355

Rubatto D, Gebauer D, Fanning M (1998) Jurassic formation and Eocene subduction of the Zermatt–Saas–Fee ophiolites: implications for the geodynamic evolution of the Central and Western Alps. Contrib Miner Petrol 132:269–287

Rutter E, Brodie K, James T, Burlini L (2007) Large-scale folding in the upper part of the Ivrea-Verbano zone, NW Italy. J Struct Geol 29:1–17

Sambridge MS, Compston W (1994) Mixture modeling of multi-component data sets with application to ion-probe zircon ages. Earth Planet Sci Lett 128:373–390

Schaltegger U, Desmurs L, Manatschal G, Müntener O, Meier M, Frank M, Bernoulli D (2002) The transition from rifting to sea-floor spreading within a magma-poor rifted margin: field and isotopic constraints. Terra Nova 14:156–162

Schaltegger U, Ulianov A, Müntener O, Ovtcharova M, Peytcheva I, Vonlanthen P, Vennemann T, Antognini M, Girlanda F (2015) Megacrystic zircon with planar fractures in miaskite-type nepheline pegmatites formed at high pressures in the lower crust (Ivrea Zone, southern Alps, Switzerland). Am Mineral 100:83–94

Schmid SM, Zingg A, Handy M (1987) The kinematics of movements along the Insubric Line and the emplacement of the Ivrea Zone. Tectonophysics 135:47–66

Schmitz MD, Bowring SA (2003) Constraints on the thermal evolution of continental lithosphere from U–Pb accessory mineral thermochronometry of lower crustal xenoliths, southern Africa. Contrib Miner Petrol 144:592–618

Schnetger B (1994) Partial melting during the evolution of the amphibolite-facies to granulite-facies gneisses of the Ivrea Zone, northern Italy. Chem Geol 113:71–101

Siegesmund S, Layer P, Dunkl I, Vollbrecht A, Steenken A, Wemmer K, Ahrendt H (2008) Exhumation and deformation history of the lower crustal section of the Valstrona di Omegna in the Ivrea Zone, southern Alps, Tectonic Aspects of the Alpine-Dinaride-Carpathian System. Geol Soc Lond Spec Publ 298:45–68

Sills JD, Tarney J (1984) Petrogenesis and tectonic significance of amphibolites interlayered with meta-sedimentary gneisses in the Ivrea Zone, southern Alps, northwest Italy. Tectonophysics 107:187–206

Sinigoi S, Antonini P, Demarchi G, Longinell A, Mazzucchelli M, Negrini L, Rivalenti G (1991) Interactions of mantle and crustal magmas in the southern part of the Ivrea Zone (Italy). Contrib Miner Petrol 108:385–395

Sinigoi S, Quick JE, Clemens-Knott D, Mayer A, Demarchi G, Mazzucchelli M, Negrini L, Rivalenti G (1994) Chemical evolution of a large mafic intrusion in the lower crust, Ivrea-Verbano Zone, northern Italy. J Geophy Res Solid Earth 99:21575–21590

Sinigoi S, Quick JE, Mayer A, Budahn J (1996) Influence of stretching and density contrasts on the chemical evolution of continental magmas: an example from the Ivrea-Verbano zone. Contrib Miner Petrol 123:238–250

Sinigoi S, Quick JE, Demarchi G, Klötzli U (2011) The role of crustal fertility in the generation of large silicic magmatic systems triggered by intrusion of mantle magma in the deep crust. Contrib Miner Petrol 162:691–707

Smye AJ, Stockli DF (2014) Rutile U–Pb age depth profiling: a continuous record of lithospheric thermal evolution. Earth Planet Sci Lett 408:171–182

Spencer KJ, Hacker BR, Kylander-Clark ARC, Andersen TB, Cottle JM, Stearns MA, Poletti JE, Seward GGE (2013) Campaign-style titanite U-Pb dating by laser-ablation ICP: implications for crustal flow, phase transformations and titanite closure. Chem Geol 341:84–101

Stacey JS, Kramers JD (1975) Approximation of terrestrial lead isotope evolution by a two-stage model. Earth Planet Sci Lett 26:207–221

Stähle V, Frenzel G, Kober B, Michard A, Puchelt H, Schneider W (1990) Zircon syenite pegmatites in the Finero peridotite (Ivrea Zone): evidence for a syenite from a mantle source. Earth Planet Sci Lett 101:196–205

Stähle V, Frenzel G, Hess JC, Saupé F, Schmidt ST, Schneider W (2001) Permian metabasalt and Triassic alkaline dykes in the northern Ivrea zone: clues to the post-Variscan geodynamic evolution of the Southern Alps. Schweiz Mineral Petrogr Mitt 81:1–21

Taylor R, Clark C, Reddy SM (2012) The effect of grain orientation on secondary ion mass spectrometry (SIMS) analysis of rutile. Chem Geol 300:81–87

Tera F, Wasserburg J (1972) U-Th-Pb systematics in three Apollo 14 basalts and the problem of initial Pb in lunar rocks. Earth Planet Sci Lett 14(3):281–304

Tribuzio R, Thirlwall MF, Vannucci R (2004) Origin of the gabbro-peridotite association from the Northern Apennine Ophiolites (Italy). J Petrol 45:1109–1124

Vacherat A, Mouthereau F, Pik R, Bernet M, Gautheron C, Masini E, Le Pourhiet L, Tibari B, Lahfid A (2014) Thermal imprint of rift-related processes in orogens as recorded in the Pyrenees. Earth Planet Sci Lett 408:296–306

Vavra G, Gebauer D, Schmid R, Compston W (1996) Multiple zircon growth and recrystallization during polyphase Late Carboniferous to Triassic metamorphism in granulites of the Ivrea Zone (Southern Alps): an ion microprobe (SHRIMP) study. Contrib Miner Petrol 122:337–358

Vavra G, Schmid R, Gebauer D (1999) Internal morphology, habit and U-Th-Pb microanalysis of amphibolite-to-granulite facies zircons: geochronology of the Ivrea Zone (Southern Alps). Contrib Miner Petrol 134:380–404

Villa IM (1998) Isotopic closure. Terra Nova 10:42–47

Villa IM, Grobéty B, Kelley SP, Trigila R, Wieler R (1996) Assessing Ar transport paths and mechanisms in the McClure Mountains hornblende. Contrib Miner Petrol 126:67–80

Voshage H, Hofmann AW, Mazzucchelli M, Rivalenti G, Sinigoi S, Raczek I, Demarchi G (1990) Isotopic evidence from the Ivrea Zone for a hybrid lower crust formed by magmatic underplating. Nature 347:731–736

Vry JK, Baker JA (2006) LA-MC-ICPMS Pb-Pb dating of rutile from slowly cooled granulites: confirmation of the high closure temperature for Pb diffusion in rutile. Geochim Cosmochim Acta 70:1807–1820

Whitney DL, Evans BW (2010) Abbreviations for names of rock-forming minerals. Am Mineral 95:185–187

Williams IS (1998) U–Th–Pb geochronology by ion microprobe. In: McKibben MA, Shanks III WC, Ridley WI (eds) Applications of microanalytical techniques to understanding mineralizing processes, Reviews in Economic Geology 7, pp 1–35

Wolff R, Dunkl I, Kiesselbach G, Wemmer K, Siegesmund S (2012) Thermochronological constraints on the multiphase exhumation history of the Ivrea-Verbano Zone of the Southern Alps. Tectonophysics 579:104–117

Zack T, Stockli DF, Luvizotto GL, Barth MG, Belousova E, Wolfe MR, Hinton RW (2011) In situ U–Pb rutile dating by LA-ICP-MS: ^{208}Pb correction and prospects for geological applications. Contrib Miner Petrol 162:515–530

Zanetti A, Mazzucchelli M, Sinigoi S, Giovanardi T, Peressini G, Fanning M (2013) SHRIMP U-Pb Zircon Triassic Intrusion Age of

the Finero Mafic Complex (Ivrea-Verbano Zone, Western Alps) and its Geodynamic Implications. J Petrol 54:2235–2265

Zingg A (1980) Regional Metamorphism in the Ivrea Zone (Southern Alps, N-Italy): field and microscopic investigations. Schweiz Mineral Petrogr Mitt 60:153–179

Zingg A, Handy MR, Hunziker JC, Schmid SM (1990) Tectono-metamorphic history of the Ivrea Zone and its relationship to the crustal evolution of the Southern Alps. Tectonophysics 182:169–192